Air Quality, Atmosphere & Health (2024) 17:2277–2305
https://doi.org/10.1007/s11869-024-01573-8

Analyses of industrial air pollution and long-term health risk using different dispersion models and WRF physics parameters

Omer Mert Bayraktar[1] · **Atilla Mutlu**[2]

Received: 27 December 2023 / Accepted: 11 April 2024 / Published online: 9 May 2024

Abstract

This study consists of three main sections. The first section delves into a performance analysis centered around modeling PM_{10}, NOx, and CO emissions from a cement factory. It examines the effectiveness of various factors, including meteorological data, physics models, and air quality dispersion models, in producing accurate results for atmospheric simulations. The second section covers the dispersion direction and concentrations obtained by visualizing the dispersion maps. The third section covers an analysis of heavy metals emitted from the facility, taking into account potential risks in the region such as cancer, acute and chronic effects, and long-term respiratory risks. This study made use of meteorological models (WRF, AERMET, and CALMET), air quality dispersion models (AERMOD and CALPUFF), a health risk analysis model (HARP), and various sub-models (MMIF and CALWRF). Satellite meteorological data were obtained from NCEP and ERA, with the majority of meteorological data based on the Global Data Assimilation System (GDAS)/Final Operational Global Analysis (FNL) from Global Tropospheric Analyses and Forecast Grids used for the WRF model. In the daily results, AERMOD showed the highest concentration values, but CALPUFF had greater concentrations throughout the annual period. The winter season had the highest concentrations of pollutants. Although there are differences among the physics models used in this research, the conclusions produced are consistent. Analysis of the data from the HARP model suggested that cancer risk levels exceeded the threshold of one person per million. However, the proportion of exceedance instances is rather small in comparison to the receptor points.

Keywords PM_{10} · NOx · CO · AERMOD · CALPUFF · WRF · HARP · cancer risk

Introduction

Studies on air pollution from past to present revealed that chemical, biological, or organic and inorganic substances released into the air as a result of human activities were extremely dangerous for living things and the environmental ecosystem (Sierra-Vargas and Teran 2012; Dianat et al. 2016; Li et al. 2016; Maleki et al. 2016; Rao et al. 2017; Cipriani et al. 2018; Zhao et al. 2019). Every year, millions of people die from the acute and chronic effects of pollutants in the air as well as extremely fatal health problems such as cancer (Goldberg et al. 2008; Kampa and Castanas 2008; Guarnieri and Balmes 2014; Guan et al. 2016). Emissions released to the environment as a result of the activity of numerous factors, such as industrialization, pandemic, global climate change, and human activities, have become an important topic in terms of air pollution for researchers (IPCC 2007; Zhang and Batterman 2013; Kinney 2018; Fu et al. 2020).

With the increasing number of people living in our world, the need for materials increases as a consequence of the increase in the need for raw materials. Different building materials are used to meet this demand. Among these building materials, cement which, in addition to being a durable, long-lasting, and low-cost building material, meets the needs of many sectors and is widely used, thereby increasing its production. On examination of the cement-producing countries in the world, China, America, and India stand out as the largest producers, while Vietnam and Turkey follow this ranking (USGS 2023). Despite the efforts to keep emissions under control in the cement factories, these factories still

✉ Omer Mert Bayraktar
mertbayraktar585@gmail.com

1 Department of Environmental Engineering, College of Engineering, Kocaeli University, İzmit, Turkey

2 Department of Environmental Engineering, College of Engineering, Balikesir University, Balıkesir, Turkey

account for approximately 5-7% of the total carbon dioxide (CO2) and 3% of the total greenhouse gas effect (Hendriks et al. 1998; Galvez-Martos and Schoenberger 2014; Çankaya and Pekey 2019; Raffetti et al. 2019). It also causes the release of compounds such as sulfur dioxide (SO_2), particulate matter (PM), volatile organic compounds (VOC), carbon monoxide (CO), nitrogen oxide (NOx), sulfur compounds, ammonium (NH_3), hydrogen chloride (HCl), heavy metals, and hydrogen fluoride (HF) (Chinyama 2011; Schorcht et al. 2013; Mosca et al. 2014; Leone et al. 2016; Shen et al. 2017). PM, which is the main intermediary product in cement production activities, can be found in different sizes depending on the particle size and diameter, especially particles below 10 µm, both causes respiratory diseases and increases the mortality rate (Zanobetti and Schwartz 2009; Stanek et al. 2011; Anderson et al. 2012). NOx, another gas that has an important role in atmospheric chemistry, is an important pollutant that must be kept under control as it plays a role in the formation of inorganic aerosols and can cause negative effects on human health (Mueller et al. 2004; Wang et al. 2011; Zhao et al. 2013; Salva et al. 2023). Emissions can enter the human body directly through the respiratory tract as a result of their dispersion into the atmosphere, or indirectly through penetration into soil and water (Schuhmacher et al. 2004).

The World Health Organization (WHO) has determined certain limit values to control the damage caused by emissions that may negatively affect the environment and living life. On examination of the studies, Miller and Moore (2020) revealed the climate, health, and economic impact of air pollution emissions caused by cement production. Rauf et al. (2021) emphasized that the health effects of emissions released from a cement factory in Indonesia on the residential areas were below the threshold limits of risk for respiratory non-carcinogenic risks and that studies beware of total suspended emissions (TSP). The study of Leone et al. (2016) compared the simulation of PM_{10} pollutants originating from two cement factories in Caserta, Italy for a whole year with air quality monitoring station (AQMS) data in the region by means of the Second-order Closure Integrated Puff (SCIPUFF) model and revealed that while both simulation and measured data exhibited high levels in winter, low levels in autumn and spring, and lowest levels in summer and the cement was highlighted to be responsible for the deterioration of air quality in the city of Caserta. Bildirici (2020), in the study conducted on the effects of production, death rate, economic growth, and air pollution relations in China, India, Brazil, America, and Turkey, which are the largest cement-producing countries in the world, mentioned that the air pollution and the mortality rates are increased as a result of the increase in the cement production and highlighted that CO2 and mortality rates could not be reduced without reducing the cement production. In a study determining the causes and effects of air pollution in Turkey, Bayram et al. (2006) specified the causes as cement, iron and steel industry, and thermal power plants, also including the transportation and domestic fuel sources, and the importance of the development of renewable energy sources was emphasized.

The best way to reduce pollution and harm caused by pollutants is to keep emissions under control. For this purpose, a number of models have been developed through numerous methods and theories to predict the resulting pollution, and the models are expected to meet criteria such as performance, reliability, and compatibility (Weil et al. 1992). Air pollution has been recognised as a major concern by many studies, and at the same time, meteorological, geographical, and emissions changes affect air pollution on both regional and global scales. (Mayer 1999; Arnold et al. 2004; Ilten and Selici 2008; Fenger 2009; Ramanathan and Feng 2009). Air pollution affects pollutant release depending on the geographical land structure, pollutant type, and the effect of atmospheric events (Kesarkar et al. 2007; Stein et al. 2007). As atmospheric weather events can be affected by many conditions and situations, unlike fixed factors such as geographical conditions, their analysis, and acquirement of realistic results are very difficult. Therefore, various physics models have been developed to analyze weather simulation (Gbode et al. 2019; Tian et al. 2021). A "mesoscale numerical model" was developed to analyze such complex calculations and perform full-time calculations (Molinari and Dudek 1992; Song et al. 2009; Ching et al. 2014; Fustos-Toribio et al. 2022; Valappil et al. 2023). An example of these models, the Weather Research and Forecasting (WRF) model, is a medium-scale weather forecasting model that enables researchers around the world to obtain past, future, and instantaneous meteorological data (Skamarock et al. 2019). On examination of the studies prepared with the WRF model, the model seems to be used in many different fields and studies such as hurricanes, floods, precipitation, heat wave, wind, and solar energy (Davis et al. 2008; Lara-Fanego et al. 2012; Efstathiou et al. 2013; Eltahan and Magooda 2018; Fustos-Toribio et al. 2022; Tuy et al. 2022; Valappil et al. 2023).

In this study, we modeled PM_{10}, NOx, and CO emissions released from a cement plant. We compared the performance of meteorological data, physics models, and air quality dispersion models to determine which option yielded the best results in atmospheric simulations. Additionally, we examined the long-term risks posed by heavy metals and PM_{10} emissions from the plant, as well as the potential cancer, acute, and chronic respiratory risks in the vicinity.

Study area

The study was conducted in the Balikesir region, located in the northwestern region of Turkey. Balikesir is a city that hosts multiple activities such as tourism, agricultural, and industrial activities. The city, with approximately 1.3 million people, has a higher population in the summer months due to being a tourism region (TUIK 2023). The general characteristics of the Balikesir region include a continental climate in the inner regions and a Mediterranean climate in the coastal area. In addition to hosting Turkey's most important mountains, the city center is surrounded by mountains in the north, northwest, and southwest parts due to its unique geographical structure, as seen on the relief map in Fig. 1. As an effect of such land conditions, the warm air rising from the ground encounters hot air higher than itself, preventing the air coming from the lower level from dispersing and remaining suspended. Consequently, the so-called inversion layer emerges and can lead to serious health problems (Ahrens 2015; Trinh et al. 2019). In particular, consumption of fossil fuels and industrial activities increase this risk for settlements in mountainous terrain such as the central region of Balikesir (MOEUCC 2020; Mutlu and Bayraktar 2021). The long-term dominant wind direction of the region was emphasized to be northern winds by studies (Mutlu and Bayraktar 2021). Two AQMS measure the composition of existing air in the city center. This study referred to these stations as A-AQMS (Central Station) and B-AQMS (Bahcelievler Station). The stations were established to test the air quality of Balikesir City Centre and measure the limit exceedances. Considering the placement of stations, the Central AQMS is positioned inside the residential center region, therefore monitoring background emissions from domestic heating and vehicles. In this station, PM_{10}, NOx, and CO ambient concentrations have been monitored by employing "Environment SA-MP101M", "Environment-SA-AC32e", and "Environment-SA-CO12e". In addition, the instruments measure PM, NOx, and CO using beta-ray, chemiluminescence, and non-dispersive infrared (NDIR) methods, respectively. The second station, Bahcelievler, is distant from downtown, the major route, and mostly sources concerned with background and heating emissions. The "Metone BAM1020" and "Teledyne API 200E" instruments are utilized at the Bahcelievler station to measure ambient concentrations using the same method as Central AQMS for PM_{10} and NOx. Both AQMS are situated in the upwind region of the facility, with the center midpoint of the facility being assessed in this study positioned at a distance of 4.6 km for the center AQMS and 3.2 km for the Bahcelievler AQMS.

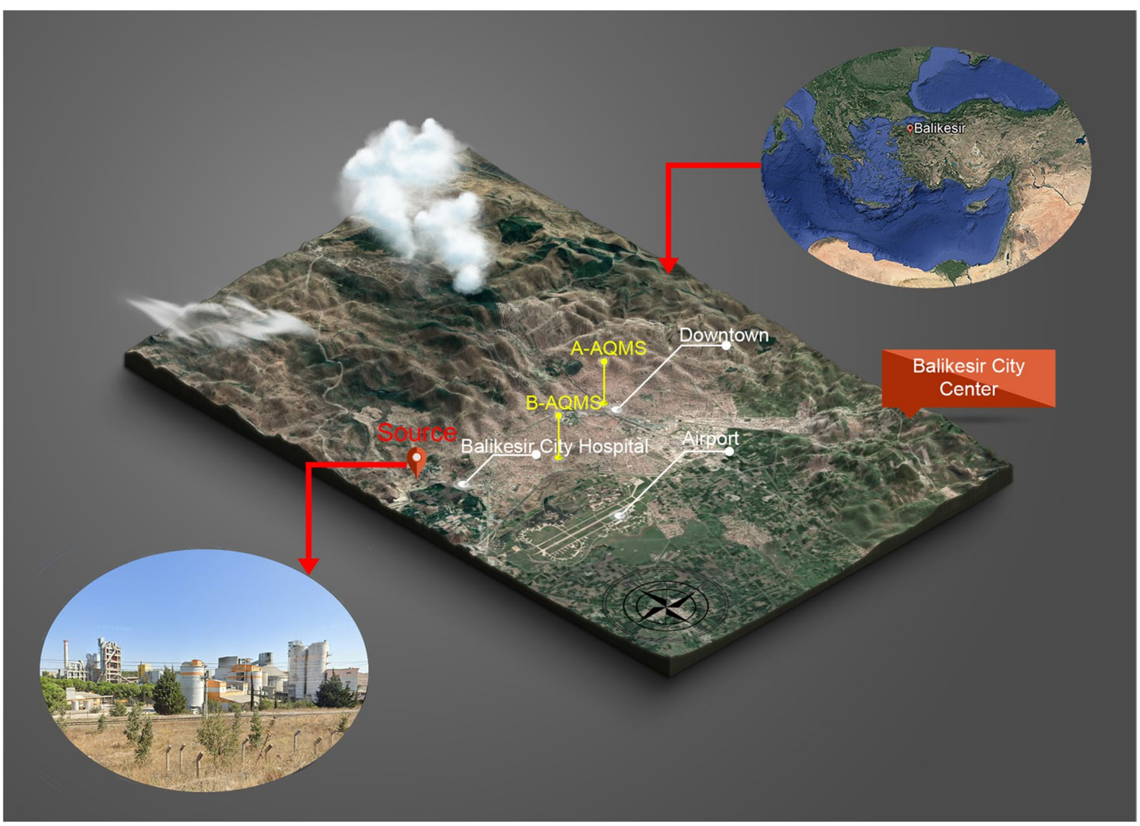

Fig. 1 Study area

While the facility is located in the center of Balikesir province in the Marmara region of Turkey, it continues its operations in the south of the city center. There are residential areas and a 500-bed Balikesir Central Hospital approximately 1 km away from the facility. The facility blends clay, limestone, gypsum, and iron ore raw materials from cement production quarries through certain processes, and consequently produces, packages, and ships the final product. The facility produces approximately 2 million tons of clinker and cement and sells the same to the domestic and foreign markets (EIA Report 2014). The facility possesses an open area of 1,140,000 m^2 and a closed area of 25,630 m^2. The facility runs full-time throughout the year and employs around 150 people. During its operation, PM_{10}, NOx, CO, and heavy metals are emitted from the plant owing to these activities.

Data and methodology

Emission inventory

Cement manufacturing processes emit PM, NOx, CO, SO2, VOCs, and heavy metals pollutants. (Zhang et al. 2015; Wang and Chen 2016; Li et al. 2018; Adeniran et al. 2019; Parlak et al. 2023). This study measured emission data of PM_{10}, NOx, CO, SO_2, and heavy metals from the facility. Background emission input was not included in this study. Emission measurements were carried out at regular intervals between February 16 and 23, 2021. The simulation period in this study was also 2021. SO_2 was neglected for this investigation because SO_2 concentrations did not exceed the official limits levels. Modelled and measured NOx pollutants at the plant are the sum of NO and NO_2. Flue gas basic parameters of the ISO 10780 method were utilised to measure basic parameters. Emission sources were monitored utilising the PM_{10} "EPA 40 Part 50", NOx "EPA CTM 022", and CO "ISO 12039" techniques for this investigation. The air quality model utilized three distinct emission types in this study: point, line, and area sources. The facility under investigation comprises a total of 45 active chimneys, with primary emissions originating from the farine mill (Stack 1), coal mill stack (Stack 2), and vertical cement mill (Stack 3). The remaining 42 chimneys exhibit significantly lower emission levels. Therefore, 42 operational chimneys were integrated with a representative stack (Stack 4) to develop air quality models for this study (Mutlu 2020). Additionally, storage, bulk, and loading activities were considered part of the area's sources. Vehicles facilitate the transportation of raw materials within the facility, covering an estimated distance of 820 meters from the source line. Various measures such as bag filters, dust collector cyclones, electrostatic dust collectors, and watering of plant roadways are employed to mitigate PM emissions released by the facility. The study presents annual emissions data for carcinogenic heavy metals, fine dust (PM_{10}), and other pollutants (NO, NO_2, and CO) from point emission sources in Table 1. Furthermore, Table 2 provides information on emissions from other line and area sources.

Apart from the cement factory located in Balikesir, which has been selected for this research, there are structured industrial zones and numerous firms as well as residential neighbourhoods in the region. It is revealed that, while looking at the downtown location in Fig. 1, domestic settlements are more concentrated in the city center and B-AQMS locations. Therefore, air pollution produced by heating occurs in this location, and it was noted that CO and SO_2 pollutants

Table 1 Annual air emissions from the analyzed point emission sources

Type of pollutants	Name of pollutants	Point sources			
		Stack 1 (kg/yr)	Stack 2 (kg/yr)	Stack 3 (kg/yr)	Stack 4 (kg/yr)
Heavy metal	Antimony	14.1	-	-	1.4
	Arsenic	22.2	0.9	0.5	11.8
	Copper	10	1.8	0.5	15
	Cadmium	-	0.9	-	0.5
	Cobalt	7.7	-	0.5	2.3
	Chromium	43.5	0.5	0.5	16.3
	Lead	35.8	3.2	0.5	11.3
	Mangan	7.7	1.8	0.9	43.1
	Thallium	-	1.4	-	0.5
	Vanadium	21.3	1.8	0.5	10.4
Emission	PM_{10}	7621	754	797	17695
	NO	721824	90404	-	-
	NO_2	11826	2190	736	-
	CO	377206	47041	-	-

Table 2 Area and line sources

Name of pollutants	Type of process	Type of sources	Emission rates (kg/yr)
PM_{10}	Area	Storage area	2745
		Bulk area	8451
		Loading area	8451
	Line	The transportation of raw materials to the facility	32050

had the maximum values in February, which was the heating season (Mutlu and Bayraktar 2021). Linear emissions from vehicles, an average of 4600 vehicles pass through the downtown location during the morning peak hours (Mutlu 2019). At the same time, A-AQMS is positioned in this location, where the heaviest traffic passes. In addition, B-AQMS is distant from the city center's main road line. The industrial zones in the centre of Balikesir can be classified into two places. The industrial zone is situated in the northeast of the Downton area, while the other is located in the southwest relative to the site of the cement factory utilised for the study in Fig. 1. At the time of this study, insufficient research existed regarding the air pollution emanating from these structured industrial zones; consequently, they were not included in the model inputs.

Meteorological data and WRF domain

Meteorological data were obtained from satellite data for the WRF-ARW model and local stations for the AERMET and CALMET models. Surface meteorological data were obtained from Balikesir Airport station, which was 4.5 km away from the center of the cartesian for chosen grids, and wind speed, wind direction, temperature, pressure, humidity, cloud cover, and cloud height data sources were provided hourly. Upper air meteorological data were obtained from Istanbul Kartal Regional Station, approximately 180 km away, with pressure, altitude, temperature, wind speed, and wind direction data in 12-hour periods. Meteorological data from the stations were prepared using AERMET and CALMET models. Meteorological data from the satellite were obtained from NCEP and ERA. The majority of meteorological data was used for the WRF model from Global Tropospheric Analyses and Forecast Grids (ds083.3) data via the Global Data Assimilation System (GDAS)/The Final Operational Global Analysis (FNL) (NCEP 2015). Although the data set was from NCEP, which measured nearly 35 meteorological parameters in 0.25 grid and 6-hour periods, due to the absence of sea surface temperature (SST) data in the ds083.3 meteorological data set, this data was obtained through the Fifth Generation of European Re-Analysis (ERA5). ERA5, developed by the European Center for Medium-Range Weather Forecasts (ECMWF), produces a dataset containing atmospheric, surface, and ocean climate data (Hersbach et al. 2020; Muñoz-Sabater et al. 2021). The model domain area is divided into two types: internal and external domains, taking Balikesir City center as the origin point. The outer domain of the model was kept as wide as possible and more data sets were tried to be included in the model. The outer domain was created with a total of 70 grids in an area of 2100 x 2100 km with a distance range of 30 km^2. The inner domain was created with a total of 40 grids in an area of 400 x 400 km with a grid distance of 10 km^2. The meteorological model domain area is presented in Fig. 2.

WRF model and physics

The WRF model, which was developed as a result of the collaboration of many institutions and organizations such as the National Center for Atmospheric Research (NCAR), the National Centers for Environmental Prediction (NCEP), the National Oceanic and Atmospheric Administration (NOAA), the Forecast Systems Laboratory (FSL), the Air Force Weather Agency (AFWA), the University of Oklahoma and the Federal Aviation Administration (FAA), and the Naval Research Laboratory, is still being developed and new versions continue to be developed (Michalakes et al. 2005; Afzali et al. 2017). In its simplest definition, the model tries to approximate weather events in the atmosphere to real data through numerical calculations. The occurrence of atmospheric weather events depends on many factors and conditions. It is, therefore, difficult to follow and examine weather events. Researchers have developed various physics methods by introducing specific calculation methods to analyze such events. Microphysics (MP), cumulus, and planetary boundary layer (PBL) were emphasized to be important for predicting weather events in terms of achieving realistic prediction and simulation (Boadh et al. 2016; Gbode et al. 2019). Many academics have worked with WRF to improve the results of the model and optimize it for the desired purpose. Bukovsky and Karoly (2009) analyzed the 4-month precipitation period via the convective parameterization scheme using SST data, and as a result, the simulations used with SST data achieved the best results; additionally, while many researchers benefited from SST data as well (Jung et al. 2012; Shimada et al. 2015; Martinez et al. 2019; Tuy et al. 2022). Evans et al. (2012) analyzed the physics options suitable for the region by using different PBL, cumulus, short wave (SW), long wave (LW), and MP schemes to analyze the rain season in Australia. Duzenli et al. (2021) achieved realistic results with the WRF model by using different physics options, ERA5, and, Global Forecast System (GFS) data for the analysis of flood events taking place in the summer and autumn periods in the eastern Black Sea

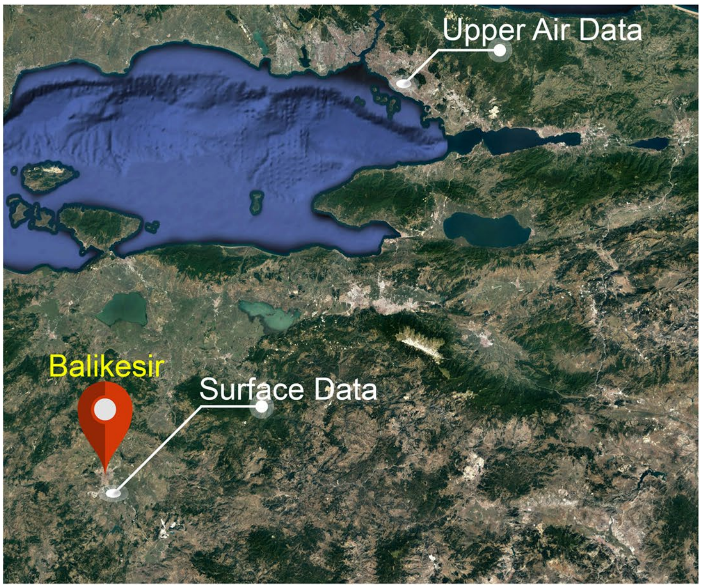

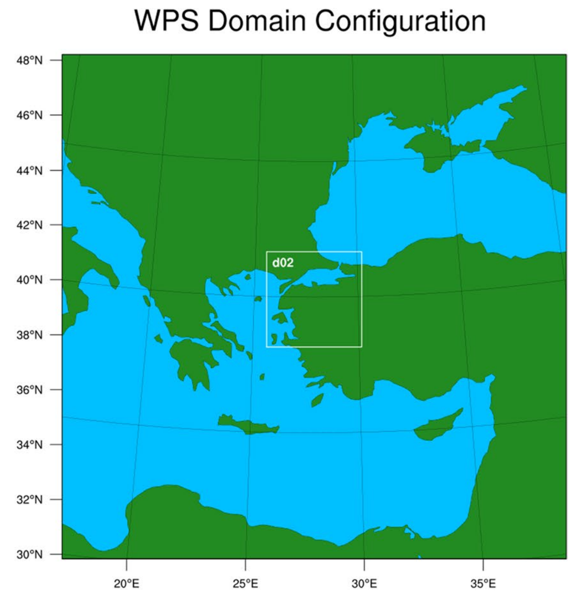

Fig. 2 Meteorological stations and WRF domain

and Mediterranean regions in Turkey, despite stating the possibility of reaching better results with SST data. Boadh et al. (2016) stated that PBL had an important place in wind circulation for transporting energy in the atmosphere, and suggested Yonsei University (YSU) and Mellor-Yamada-Nakanishi and Niino Level 2.5 PBL (MYNN2) for studies that can be used for air pollution dispersion. Afzali et al. (2017) examined the air quality dispersion of the region with AERMOD, using PM_{10}, NO_2, and SO_2 pollutants released as a result of multiple industrial activities in Malaysia as well as surface and upper air meteorological data obtained from the WRF model. Rzeszutek et al. (2023) studied the WRF model with other air quality dispersion models (AERMOD, ADMS, and CALPUFF) for under 50 km as a consequence of temperature and wind speed simulations that were sensitive to the location of the grid area, and the WRF domain size created less inaccuracy with high resolutions.

This study aims to obtain the best results for the study area by testing different physics options with the WRF model. Depending on this situation, simulations were carried out on seven different scenarios. While selecting physics options, previously used physics infrastructures with the best results were used and studies conducted in the same geography were also included. The scenarios were prepared for the WRF model. The selected physical properties and the rationale based on previous studies according to the ensemble numbers (EN) provided in Table 3 are as follows: No. 1: The Thompson microphysics option, which was used as Contiguous United States (CONUS) in the WRF user guide and the WRF model input file "namelist.input" by default after model installation, was preferred and used in a variety of studies (Lo et al. 2008; Wyszogrodzki et al. 2013; Ryu et al. 2019; Ünal et al. 2019). No. 2: The WSM6 Class microphysics option recommended by "NCAR" in the 10-30 km grid range, specified in the WRF user guide regional climate was used (NCAR 2017; Skamarock et al. 2019). It was also preferred because Turkey was the region of this study and it had a frequently preferred physics infrastructure

Table 3 Physical options

Ensemble no (EN)	Microphysics	Planetary boundary layer/ Surface layer	Cumulus physics	Shortwave/Long-wave radiation physics
1	Thompson "CONUS"	MYJ/ETA	Tiedke	RRTMG/RRTMG
2	WSM6 "NCAR"	YSU/MM5	KF	CAM/CAM
3	GD	MYJ/ETA	BMJ	RRTMG/RRTMG
4	MY	MYJ/ETA	BMJ	RRTMG/RRTMG
5	Eta Ferier	MYJ/ETA	KF	Dudhia/RRTMG
6	WSM3	YSU/MM5	Grell	RRTMG/RRTMG
7	LIN	Bougeult/ETA	Grell	RRTMG/RRTMG

for different studies (Patel et al. 2019; Özen et al. 2021). No. 3: Gbode et al. (2019) compared 27 different physics combinations to analyze the African monsoon rain regime and used Goddard (GD) microphysics, one of the options that provided the best value in terms of model skill score, while Hines and Bromwich (2008) used MM5 and WRF models and GD microphysics for polar weather research as the same physics model. No. 4: Morrison and Milbrandt (2011) examined precipitation, storm, and cold pool strength activities between Morison and Milbrandt-Yau microphysics using the WRF model. No. 5: Efstathiou et al. (2013) carried out large-scale simulations for heavy rainfall situations, especially by evaluating different microphysics options and using Eta Ferrier microphysics. No. 6: Mahala et al. (2015) and Eltahan and Magooda (2018) used WRF-single-moment-microphysics Class 3 (WSM3) for atmospheric events such as excessive rain and severe storm formation. No. 7: Patel et al. (2019) evaluated different physics options to predict floods in the coastal region and stated that Lin and Grell's physics options significantly reduced the bias rate. The physics schemes prepared for this study are presented in Table 3.

Due to the width of the study area and the density of the resulting data set, WRF outputs are in compressed files. Libraries developed from programming languages such as WRF-python help to extract data from these files. As another option, sub-models have been developed to make the necessary data for the models ready for use. Especially, models such as The Mesoscale Model Interface Program (MMIF) and CALPUF-WRF (CALWRF) are useful tools for air quality dispersion models to capture the meteorological data needed for AERMOD and CALPUFF and the data prepared in the WRF model. For this study, MMIF and CALWRF models were used and converted into a data set format that air quality dispersion models can understand. In addition, CALMET has been used to re-run the CALWRF outputs. CALMET has optimized the discrepancies between the WRF and CALPUFF meteorological domain areas because they differ from one another in this study. The required bases for the simulation were WRF pre-processing system (WPS), version 4.3.1 and WRF-ARW, version 4.3.3.

Air quality dispersion models

While many different models have been used for many fields and purposes from past to present for air quality dispersion models, models have been developed with new methods and technological developments (Hanna et al. 2001; Gulliver and Briggs 2011; Holnicki et al. 2016; Ruiz-Arias et al. 2016). While these predictions were prepared with manual calculations and limited data sets in the past, with technological developments today, it has become possible to obtain meteorological data from satellites and results closest to reality with different methods and calculation methods. Consequently, different air quality dispersion models have been developed depending on the needs of different institutions, organizations, and researchers. Examples of these models include AERMOD and CALPUFF. Both models are used by many researchers and validated by organizations (US EPA 2000; FLAG 2010; De Melo et al. 2012; Tartakovsky et al. 2013; US EPA 2019). Although both types fundamentally perform the same job, they have variances based on the region of application and method of function.

AERMOD model is generally used for distances between 0-50 km whereas the CALPUFF model is mainly used to represent lengths of 50 km or greater. The EPA does not recommend < 50 km as near-field applications for the CALPUFF model (Harnett et al. 2008; Jittra et al. 2015). On the other hand, the CALPUFF model has also been used in near-field applications for long-term dispersion models where complicated flows caused by complex terrain and land use variations are considered significant with emphasis on model performance, validation, and exposure levels (MacIntosh et al. 2010; Cui et al. 2011; Dresser and Huizer 2011; Ghannam and El-Fadel 2013). When the near-field applications using the CALPUF models were examined, there were variances in the study distances utilised for the models; they were used to estimate emission distributions for research regions under 50 km in many studies (Scire et al. 2000; Abdul-Wahab et al. 2011; Tartakovsky et al. 2013; Gulia et al. 2015; Afzali et al. 2017; Demirarslan et al. 2017; Rzeszutek et al. 2023; Zeydan and Karademïr 2023). On examination of these studies, Emert et al. (2024) analysed the air quality distributions of PM_{10} and $PM_{2.5}$ pollution from beef cattle feedlots using the CALPUFF model, which included the hot months and indicated that modelled pollutants exceeded the safe limit values for humans. Eslamidoost et al. (2023) investigated a gas refinery in Iran, which has a capacity of approximately seven hundred twenty billion cubic metres of gas, using the AERMOD model and concluded that there was no exceedance of the EPA limit value. In the same region, Rashidifard et al. (2018) simulated CO emissions using AERMOD and CALPUFF models from a steel industry in Iran and found that AERMOD had better results than the CALPUFF model. In another research, Gulia et al. (2015) emphasised that AERMOD, which used a plume dispersion model, was less successful in calm weather conditions compared to CALPUFF.

AERMOD (AMS/EPA Regulatory Model), a prediction model that uses the algorithm based on the plume model dispersion and the Gaussian dispersion, is a model developed by the American Meteorology Society (AMS) and the United States Environmental Protection Agency (US EPA). It also has a sub-model that prepares data for AERMOD. The model, with its 2 sub-models AERMAP and AERMET, makes the terrain and meteorological data set ready for the AERMOD, and finally, the model is run after the processing of specific inputs such as building evaluation, study area, grid distances, and pollutant features through AERMOD (US EPA 2019). The CALPUFF (California Puff Model) model, developed together with the California Air Resource Board and Sigma Research Corporation, uses the Lagrangian Puff dispersion model method. The model contains multiple sub-models within itself. The fundamental models consist of TERREL, CTGPROC, MAKEGEO, and CALMET. Sub-models prepare the parts where the geographical land data set, vegetation, and meteorological data are processed for the CALPUFF model. The CALPUFF model is also an EPA-recommended model (US EPA 2000).

Risk analysis model

Hotspots Analysis and Reporting Program (HARP), developed by the California Air Resource Board and Office of Environmental Health Hazard Assessment (OEHHA), is a program that can perform toxicity analysis depending on air quality and emission characteristics (OEHHA 2009; OEHHA 2015). The HARP model is a model originally developed to control air quality and take precautions against possible risks of emissions released into the air from facilities. In addition, the HARP model was used to analyse health risk assessment using air quality models (Environ Australia 2008; Donoghue and Coffey 2014). The model calculates possible risk scenarios using AERMOD outputs and toxic pollutants. In addition, the model includes different scenario options such as respiration, soil, skin, breast milk, drinking water, fish, and small and large livestock farming. The model consists of Emission inventory, Air Dispersion Modeling, and Risk assessment tools. The model can produce the required outputs with its own AERMOD module, and the dispersion results produced by AERMOD can also be separately incorporated into the HARP model. Since the model outputs are in the plot file (PLT) data type produced by the AERMOD model, it is possible to prepare and use different data sets or different air quality dispersion models in this format. After the study area inputs are processed for risk analysis by the model, pollutant emissions that pose a health risk are input. After processing the operating characteristics, air quality dispersion results, and toxic characteristics of the pollutant required by the model, the exposure level (25, 35, 70 years (lifetime), etc.), analysis type (cancer, acute and chronic risk), and risk type are selected.

In this model, HARP uses several fundamental inputs to the working principle of the model, and the first necessary data is the air quality dispersion model in PLT format. In addition, background emission inputs may be combined with air quality inputs in the model. The model needs input emissions inventory (a "HARP database" for the emission risk ratio) and health risk assessment factors. Pollutant sources need their parameters (stack height and internal diameter, gas exit velocity, and UTM coordinates). Pollutant source features are also incorporated into the model (stack height and inside diameter, gas exit velocity, and coordinates). In regard to the working time of the facility, it is important to examine the health risks related to the exposed time period. Finally, the model risk scenario is chosen to examine health concerns. As a consequence, the model creates the analysis-type situations specified by the user. The computation of the model configuration differs according to the specified research scenario. Model scenarios and calculation methods are included in the guidebook, and the equation is presented below (OEHHA 2015). Daily inhalation dose (Doseair) and residential inhalation cancer risk (RISKinh_res) were used to calculate the inhalation-risk scenario. The other equalities are formulas, concentration in air (Cair), daily breathing rate normalised to body weight (BR/BW), inhalation absorption factor (A), exposure frequency (EF), inhalation cancer potency factor (CPF), age sensitivity factor for a specified age group (ASF), exposure duration (ED), averaging time for lifetime cancer risk (AT), and fraction of time spent at home (FAH) (OEHHA 2015).

$$Dose_{air} = C_{air} * \left\{ \frac{BR}{BW} \right\} * A * EF * 10^{-6} \tag{1}$$

$$RISK_{inh-res} = Dose_{air} * CPF * ASF * \frac{ED}{AT} * FAH \tag{2}$$

This study used calculation methods for the inhalation-risk scenario, but ASF, FAH, and BR/BW inputs were missing. Therefore, these inputs were utilised as the default data of the HARP model. The latest available version of the model is HARP 2, and the most current version was used for this study.

Model methodology

This study made use of meteorological models (WRF, AERMET, and CALMET), air quality dispersion models (AERMOD and CALPUFF), health risk analysis model (HARP), and various sub-models required for these models (MMIF and CALWRF). Meteorological, topographic, vegetation, and emission inputs were used as data input. The meteorological data set was provided in two different ways, i.e., satellite and local station. The majority of meteorological data sets from satellites were obtained through "NCEP GDAS/FNL 0.25 Degree Global Tropospheric Analyses and Forecast Grids". However, since SST data is not included in GDAS data, it was obtained through ERA. Both data sets available through ERA and NCEP were compatible with the WRF model and no preliminary correction was required. Due to the missing data in the local meteorological station data set, the deficiencies were eliminated by using the meteorological data of the last 5 years from surface stations that belong to 2017-2021. The completed data sets were made compatible with the air quality dispersion model with sub-models, the sub-units of the models. The Shuttle Radar Topography Mission (SRTM3) 90 m data was used for topography data in both models. Due to the differences between the models, the vegetation was processed manually in AERMOD and this dataset was used as a raster 100 m via CORINE for CALPUFF. CALPUFF is different from AERMOD in that it includes a chemical transformation process. CALPUFF can simulate secondary fine particles formed by chemical reactions in atmospheric transports (Scire et al. 2000; Zhou et al. 2003). In this study, the utilization of secondary emission input was not incorporated into the CALPUFF model. Using the satellite and local meteorological data and AERMET, CALMET, and WRF models together with the air quality dispersion models of AERMOD and CALPUFF, we prepared eight different dispersion models, that is, the eight meteorological inputs (7 WRF + 1 Local) used by each model.

While the main emission sources released as a result of the operation of the facility were the pollutants of PM_{10}, NOx, and CO, heavy metal emissions took place as well. The models consist of line, area, and point source as source types. Air quality dispersion models were prepared on an hourly, daily, and annual basis for the entire year 2021. Model-specific input of air quality models was arranged as a Cartesian grid within an area of 15 x 15 km in 500 m grids. The model was run after the arrangement of the data for the AERMOD and CALPUFF models. Correlation analysis was carried out between the forecast data produced as a result of the simulation and the data obtained from the measurement stations at A and B-AQMS locations in Fig. 1. In the data from the stations, PM_{10}, NOx, and CO pollutants were measured with A-AQMS, while PM_{10} and NOx were measured with B-AQMS. As a result, the relationship between air quality models along with meteorological models and physics models was examined.

In the last stage, the HARP model was used to analyze the health risks of the model outputs. PLT pollutant data, which are CALPUFF and AERMOD model outputs, and heavy metal data released from the facility were added to the model as source output in Table 1. Then, within the HARP model, a risk assessment was made at a total of 962 recipient points, including possible cancer through the respiratory tract, acute and chronic risks, 70-year (lifetime) exposure, 95th risk effect, and sensitive points such as Balikesir Central Hospital. The general flow scheme of the model is presented in Fig. 3.

Data analysis results

Model-observation comparison

The model simulation content prepared for this study was prepared to cover the entire year. Since the WRF model domain used to provide meteorological data does not allow the computer hardware to operate over a long period, the one-year study period was divided into three parts, creating 4-month intervals. Sixteen different results were obtained in this period, with model outputs being created with eight

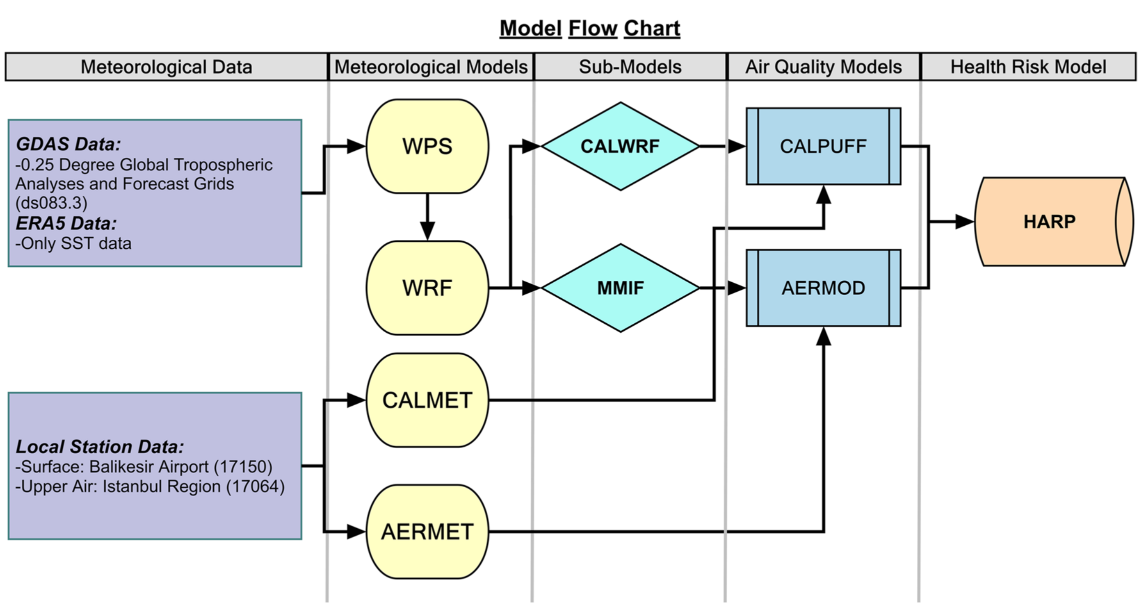

Fig. 3 Model flow chart

different meteorological inputs, i.e., hourly, daily, and annual, and two different air quality dispersion models. Within the scope of the aims of the study, the pollution levels were determined and the results between the models and the physics options were compared. There are two stations in Balikesir city center: Central Station and Bahcelievler Station. Among these stations, PM_{10}, NOx, and CO pollutants were measured at Central Station, while PM_{10} and NOx pollutants were measured at Bahcelievler Station. The characteristics of the sixteen model simulations are presented in Table 4.

On examination of the pollutant source and AQMS locations used in this study, these were observed to be located in the north and northwest of the source. In this study, Spearman correlation analysis was used because the model outputs did not exhibit normal distribution (Bishara and Hittner 2012) and was also used in many studies from CALPUFF and AERMOD (Zou et al. 2011; Ghannam and El-Fadel 2013; Hoinaski et al. 2017; Bezyk et al. 2021; Eslamidoost et al. 2022). Therefore, the location of the facility in the upwind region may cause differences between the modelled and measured station data. On examination of the correlation analysis between model results and AQMS, daily measurements at both stations exhibited higher significance than hourly measurements. The highest correlation values among pollutants were observed in the daily period. The highest correlation value among concentration was seen in NOx concentrations, followed by PM_{10} and CO, respectively. In A-AQMS, the highest correlation of daily concentrations of NOx were measured at 0.72, while in B-AQMS, they were slightly lower at 0.62. For hourly predictions, the highest correlation of NOx concentrations were 0.44 in A-AQMS and 0.39 in B-AQMS. Likewise, highest correlation of daily predicted PM_{10} levels were 0.70 in A-AQMS and 0.41 in B-AQMS, with corresponding hourly predictions of 0.43 in A-AQMS and 0.30 in B-AQMS. Maximum correlation of daily predicted CO concentrations were 0.60 in A-AQMS and 0.43 in B-AQMS. Upon evaluation, it was noted that among the WRF physics options, models No. 3 (GD) and No. 4 (MY) for daily predictions, along with model No. 5 (ETA) for hourly predictions, exhibited stronger correlation values. Conversely, models utilizing local meteorological data demonstrated lower correlation values. When the models were compared, although CALPUFF achieved better results than AERMOD, the AERMOD model also produced good results. In the correlation results, the AERMOD-NOx correlation of Bahcelievler AQMS was observed as the negative correlation of meteorological inputs. In this situation, it is anticipated that several possibilities, such as calm conditions, low wind speed, different models, chemical reactions, emission sources, and the specific factor of AQMS, may be offered as examples. Hourly and daily correlation results are presented in Fig. 4 and Fig. 5.

Chang (2003), Chang and Hanna (2004), and Hanna and Chang (2012) extensively examined the calculation procedure of model validation parameters in the performance analysis. The validation parameters, such as fractional bias (FB), assess systematic biases between observed and predicted values. A positive FB suggests an under-prediction, while a negative FB signifies an over-prediction by the model (Chang 2003; Chang and Hanna 2004; Hanna and Chang 2012). The normalized mean square error (NMSE) is the total error of the standardized values between the measured and modeled data. The factor of two (FAC2) represents the accuracy of estimating parameters within a range of two times the observed value (Hanna and Chang 2012; Irwin 2014).The normalized absolute difference (NAD) is a metric that quantifies the fractional area for mistakes according to Hanna and Chang (2012). Additionally, a "good model" must satisfy at least one component within their acceptance intervals. Thus, the acceptance intervals for these control parameters are shown in Table 5. The data utilized for validation were acquired after eliminating irrelevant and missing data to compute validation parameters such as FB, NMSE, FAC2, and NAD. In the model performance of Tables 5 and 6, accepted parameters are indicated in bold type.

In this study, air quality distribution models were created using the AERMOD and CALPUFF algorithms, incorporating hourly and daily measurements of PM_{10} and NOx from the Bahçelievler AQMS, as well as CO, PM_{10}, and NOx

Table 4 Model properties

Meteorological data	Meteorological models	Ensemble no	Air quality models	
			AERMOD	CALPUFF
GDAS/ERA5	WRF	1-CONUS	✓	✓
		2-NCAR	✓	✓
		3-GD	✓	✓
		4-MY	✓	✓
		5-Eta Ferier	✓	✓
		6-WSM3	✓	✓
		7-LIN	✓	✓
Local	AERMET/CALMET	8-Surface/Upper air	✓	✓

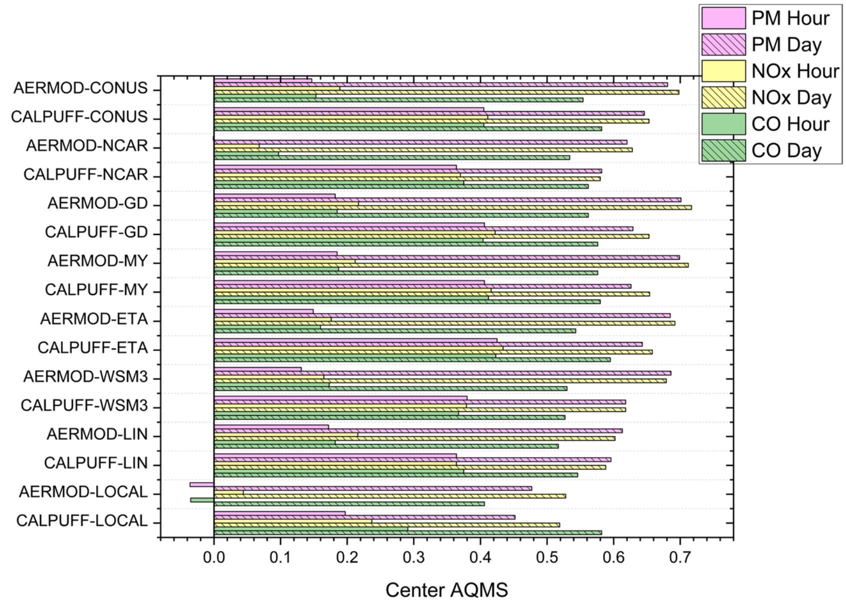

Fig. 4 Central AQMS correlation results

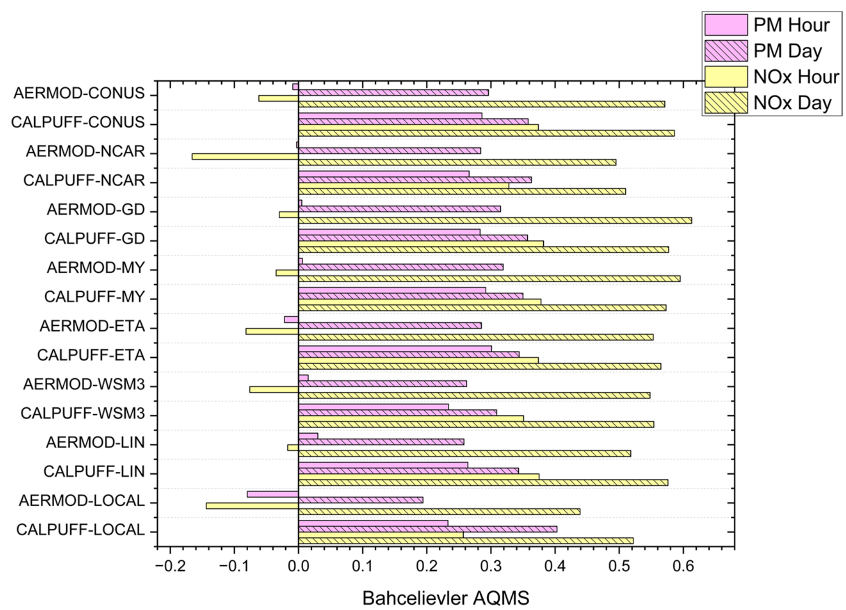

Fig. 5 Bahcelievler AQMS correlation results

pollutants measured with the Central AQMS, along with previously selected physical parameters and meteorological data. The normalized measured and modeled results were statistically analyzed to evaluate model performances. The analysis results of model performances are presented in Table 5 and Table 6 for both AQMSs.

According to the model validation results, less favorable values were observed for the FB validation parameter. On the other hand, FAC2, defined as a robust validation parameter by Chang (2003) because it is not affected by the minimum and maximum values in the datasets, is shown to be compatible with both AERMOD and CALPUFF. It has been determined that the AERMOD and CALPUFF models are more compatible with validation parameters in daily time intervals in pollutant distributions. It was found that the CO pollutant did not show intensive compatibility in modeling results like other pollutants. Further studies are required to address this issue. According to the model validation analysis results, it was determined that local meteorological data showed the least compatibility with the distribution models. It was concluded that the majority of the selected physical parameters are compatible with both AERMOD and CALPUFF.

Table 5 AERMOD and CALPUFF modeling performances on the selected physical parameters (Central AQMS)

Validation parameters	Pollutants	Periods	AERMOD/Physical parameters								CALPUFF/Physical parameters							
			CONUS	NCAR	GD	MY	ETA	WSM3	LIN	LOCAL	CONUS	NCAR	GD	MY	ETA	WSM3	LIN	LOCAL
FB [FB ≤ 0.67]	PM_{10}	Hour	1.8	1.7	1.8	1.82	1.8	1.82	1.84	1.87	1.1	1.6	1.6	1.1	1.1	1.57	1.3	1.58
		Day	0.8	1	0.84	1.2	1.05	1	1	1.2	**0.51**	1.2	0.85	**0.5**	**0.24**	**0.5**	**0.65**	0.83
	NOx	Hour	0.98	**0.64**	**-0.14**	**-0.16**	**-0.12**	**0.33**	**0.2**	1.13	**0.45**	**0.55**	0.8	**0.3**	0.73	0.7	1	0.8
		Day	0.93	1.04	0.83	0.81	0.97	0.9	**0.5**	0.88	0.8	**0.57**	0.75	0.75	0.93	**0.61**	0.87	1.06
	CO	Hour	1.15	1.55	1.5	1.45	1.16	1.47	1.3	1.8	1.56	1.6	1.6	1.57	1.59	1.6	1.7	1.65
		Day	1.14	1.3	1.05	1	1.18	1.12	0.76	1.1	1.01	0.82	0.97	0.96	1.13	0.84	1.1	1.24
NMSE [NMSE ≤ 6]	PM_{10}	Hour	38.1	26.4	37.8	44.5	38.5	43.3	48.7	67.7	7.2	17.5	18.2	7.3	6.9	16	9.3	17.5
		Day	**3.6**	**4.1**	**3.9**	**5.5**	**4.7**	**4.6**	**4.4**	6.8	**1.7**	**4.3**	**2.8**	**1.8**	**1.47**	**1.9**	**2.03**	**3.7**
	NOx	Hour	7.7	15.5	14.4	14.2	14.8	13.3	118	23.5	13.3	15.1	14.6	13.8	13.9	16.2	17.8	22.1
		Day	**3.9**	**4.01**	**3.4**	**3.3**	**4.2**	**3.5**	**2.51**	**3.8**	**2.5**	**2.2**	**2.45**	**2.3**	**3.1**	**2.2**	**3.2**	**5.4**
	CO	Hour	7.3	13.9	11.6	10.6	7.2	11.2	8.4	37.6	13.8	17.5	15.9	14.2	14.9	15	20.6	20
		Day	**4**	**4.5**	**3.4**	**3.2**	**4.3**	**3.6**	**2.1**	**3.9**	**2.7**	**2**	**2.5**	**2.5**	**3.4**	**2.1**	**3.3**	**5.7**
FAC2 [FAC2 ≥ 0.3]	PM_{10}	Hour	0.05	0.08	0.06	0.05	0.05	0.05	0.04	0.03	**0.3**	0.1	0.1	**0.3**	**0.3**	0.12	0.2	0.12
		Day	**0.4**	**0.32**	**0.4**	0.24	**0.31**	**0.3**	**0.33**	0.27	**0.6**	**0.3**	**0.4**	**0.6**	**0.79**	**0.6**	**0.5**	**0.4**
	NOx	Hour	**0.3**	**0.5**	**1.2**	**1.2**	**1.1**	**0.7**	**0.9**	**0.3**	**0.6**	**0.6**	**0.4**	**0.74**	**0.46**	**0.47**	**0.3**	**0.43**
		Day	**0.36**	**0.32**	**0.42**	**0.42**	**0.35**	**0.38**	**0.6**	**0.39**	**0.43**	**0.6**	**0.45**	**0.46**	**0.36**	**0.53**	**0.39**	**0.31**
	CO	Hour	0.27	0.13	0.14	0.16	0.27	0.15	0.21	0.05	0.12	0.1	0.11	0.12	0.11	0.12	0.1	0.09
		Day	0.27	0.23	**0.31**	**0.32**	0.26	0.28	**0.45**	**0.3**	**0.33**	**0.42**	**0.35**	**0.35**	0.28	**0.41**	**0.3**	0.24
NAD [NAD ≤ 0.5]	PM_{10}	Hour	0.9	0.85	0.9	0.91	0.9	0.9	0.92	0.94	0.54	0.8	0.8	0.55	0.55	0.78	0.7	0.79
		Day	**0.4**	**0.5**	**0.4**	0.6	**0.5**	**0.5**	**0.5**	0.6	**0.25**	0.57	**0.41**	**0.3**	**0.12**	**0.25**	**0.3**	**0.41**
	NOx	Hour	**0.49**	**0.3**	**-0.07**	**-0.08**	**-0.06**	**0.16**	**0.07**	0.56	**0.22**	**0.3**	**0.4**	**0.15**	**0.37**	**0.36**	**0.5**	**0.43**
		Day	**0.47**	0.52	**0.41**	**0.4**	**0.48**	**0.45**	**0.25**	**0.44**	**0.4**	**0.3**	**0.38**	**0.37**	**0.47**	**0.3**	**0.44**	0.53
	CO	Hour	0.57	0.77	0.75	0.73	0.58	0.74	0.65	0.9	0.8	0.82	0.81	0.78	0.79	0.79	0.84	0.83
		Day	0.57	0.62	0.53	0.52	0.59	0.56	**0.38**	0.54	0.51	**0.41**	**0.48**	**0.48**	0.56	**0.42**	0.54	0.62

FB, fractional bias, *NMSE*, normalized mean square error, *FAC*2, fraction of predictions within a factor of two of observations, *NAD*, normalized absolute difference

Table 6 AERMOD and CALPUFF modeling performances on the selected physical parameters (Bahcelievler AQMS)

Validation parameters	Pollutants	Periods	AERMOD/Physical parameters								CALPUFF/Physical parameters							
			CONUS	NCAR	GD	MY	ETA	WSM3	LIN	LOCAL	CONUS	NCAR	GD	MY	ETA	WSM3	LIN	LOCAL
FB [FB ≤ 0.67]	PM_{10}	Hour	1.82	1.76	1.8	1.81	1.85	1.81	1.86	1.82	1.29	1.23	1.59	1.27	1.48	1.39	1.22	1.31
		Day	1.13	1.25	0.7	0.84	0.98	0.87	0.88	0.7	**0.18**	**0.58**	**0.47**	**0.4**	**0.54**	**0.14**	1.04	1.26
	NOx	Hour	0.92	1.43	0.82	0.83	1.15	1.36	1.05	1.54	1.42	1.29	1.42	1.27	1.45	1.38	1.49	1.69
		Day	**0.39**	**0.46**	**0.44**	**0.53**	**0.55**	0.68	**0.19**	**0.39**	**0.19**	**0.1**	**0.22**	**0.21**	**0.57**	**0.18**	**0.36**	1.03
NMSE [NMSE ≤ 6]	PM_{10}	Hour	36.76	26.9	32.9	35.2	42.4	33.2	45.3	40.3	7.65	7.7	13.5	7.6	10.6	9.02	6.8	9.3
		Day	**5.5**	6.4	**4.6**	**4.6**	**5.2**	**4.5**	**4.4**	**4.5**	**2.08**	**2.6**	**2.43**	**2.4**	**2.62**	**2.24**	**3.7**	6.7
	NOx	Hour	10.7	18.1	10	10.1	12.3	15.8	10	24.5	16.3	13.4	16.4	12.6	17.7	15	18.3	34.5
		Day	**3.85**	**3.5**	**3.45**	**3.7**	**3.8**	**4.2**	**2.9**	**3.4**	**2.4**	**2.5**	**2.4**	**2.3**	**2.9**	**2.2**	**1.9**	**5.4**
FAC2 [FAC2 ≥ 0.3]	PM_{10}	Hour	0.05	0.06	0.05	0.05	0.04	0.05	0.04	0.05	0.21	0.24	0.12	0.22	0.15	0.18	0.24	0.21
		Day	0.28	0.23	**0.48**	**0.41**	**0.34**	**0.39**	**0.39**	**0.48**	**0.84**	**0.55**	**0.62**	**0.67**	**0.57**	**0.87**	**0.32**	0.23
	NOx	Hour	**0.37**	0.17	**0.42**	**0.42**	0.27	0.19	**0.31**	0.13	0.17	0.22	0.17	0.22	0.16	0.18	0.15	0.08
		Day	**0.67**	**0.63**	**0.64**	**0.6**	**0.57**	**0.5**	**0.82**	**0.67**	**0.83**	**0.9**	**0.8**	**0.81**	**0.6**	**0.84**	**0.7**	**0.32**
NAD [NAD ≤ 0.5]	PM_{10}	Hour	0.91	0.88	0.9	0.91	0.92	0.9	0.93	0.91	0.65	0.62	0.79	0.64	0.74	0.7	0.61	0.65
		Day	0.57	0.63	**0.35**	**0.42**	**0.49**	**0.44**	**0.44**	**0.35**	**0.09**	**0.29**	**0.24**	**0.2**	**0.27**	**0.07**	0.52	0.63
	NOx	Hour	**0.46**	0.72	**0.41**	**0.41**	0.57	0.68	0.52	0.77	0.7	0.64	0.7	0.63	0.73	0.69	0.74	0.85
		Day	**0.2**	**0.23**	**0.22**	**0.3**	**0.28**	**0.34**	**0.1**	**0.2**	**0.09**	**0.05**	**0.11**	**0.11**	**0.28**	**0.1**	**0.2**	**0.5**

FB, fractional bias, *NMSE*, normalized mean square error, *FAC2*, fraction of predictions within a factor of two of observations, *NAD*, normalized absolute difference

Inter–model comparison

On examination of the model outputs, despite observing differences in the prediction results produced by each model, the concentration difference between daily models was greater compared to annual models. While AERMOD reached the highest concentration values in daily results, CALPUFF exhibited higher concentration in annual results. Among the models, the peak concentrations of the AERMOD model were obtained with the No. 2 and No. 6 physics models, while the lowest concentration results were obtained with the No. 7 model. On examination of the CALPUFF model, a specific peak physics model was not observed for each emission. On evaluation of the annual model results of both models, the difference between them was seen to have narrowed and produced close results. The days when the models reached peak concentration were mostly during the winter season. The results of the models are presented in Tables 7, 8, and 9.

In this study, the legend features and value ranges of daily maximum and annual average dispersion maps were prepared by determining a range for each pollutant. Dispersion models of concentration recipient points were created using SURFER, a surface, a 3D map and a contouring program. Map images were prepared according to the highest pollutant concentration received by the receiving point within the specified period. On examination of the dispersion results of the models, the dispersion of pollutants in the daily model was not distributed in a certain region but had high concentrations in the central region of the pollutant source. On examination of the annual model dispersions, a more pronounced dispersion was observed than the daily model results. In particular, the dispersion of annual model pollutants was observed to be distributed towards the southern location of the source. It is thought that the major cause for this is that the dominant wind direction of the Balikesir region is the northern winds (Mutlu 2020; Mutlu and Bayraktar 2021; Bayraktar 2022; Güğül et al. 2023). When we look at the dispersion between different pollutans, the dispersion direction of NOx and CO pollutants was observed to be towards the south of the source, while the daily and annual dispersions of PM_{10} pollutants were more dominantly distributed in the center of the source. It is thought that the main reason for this is that the emission sources, which are the transport linear source and the area sources, are 10 m and < 10 m below the emission height, respectively. There are different emission sources from PM_{10} than the NOx and CO pollutants, such as NOx and CO, which do not have any area or linear type sources. Therefore, different dispersions compared to pollutants can be emphasised in the model distributions. The distributions between the models were analysed, and the daily concentrations of the AERMOD model were higher than the CALPUFF model. Daily distribution

Table 7 Results of simulation models for PM_{10} pollutant

	Time	Model	Statistics	Meteorological parameters							
				No 1	No 2	No 3	No 4	No 5	No 6	No 7	Local
PM_{10}	Daily	AERMOD ($\mu g/m^3$)	Maximum	96.132	177.347	70.153	95.575	87.832	111.644	54.764	73.560
			Median	2.984	4.901	2.902	2.957	2.746	4.191	2.871	3.885
			Minimum	0.081	0.094	0.068	0.087	0.096	0.116	0.082	0.043
			Peak date	06.01.2021	13.04.2021	02.01.2021	02.01.2021	03.04.2021	04.01.2021	02.01.2021	16.09.2021
		CALPUFF ($\mu g/m^3$)	Maximum	74.544	57.576	72.392	78.066	110.2	71.062	76.703	60.364
			Median	0.634	0.664	0.621	0.618	0.597	0.636	0.612	1.062
			Minimum	0.066	0.043	0.065	0.079	0.051	0.062	0.073	0.208
			Peak date	08.11.2021	14.11.2021	14.11.2021	20.02.2021	21.12.2021	19.09.2021	23.10.2021	24.09.2021
	Annual	AERMOD ($\mu g/m^3$)	Maximum	8.789	10.986	8.945	8.847	9.008	7.476	8.405	11.484
			Median	0.129	0.195	0.126	0.123	0.123	0.164	0.104	0.148
			Minimum	0.004	0.004	0.004	0.005	0.005	0.004	0.004	0.003
		CALPUFF ($\mu g/m^3$)	Maximum	9.127	8.630	9.875	9.376	9.704	8.227	8.248	17.449
			Median	0.050	0.036	0.043	0.048	0.046	0.038	0.045	0.105
			Minimum	0.004	0.002	0.003	0.002	0.002	0.002	0.003	0.021

Table 8 Results of simulation models for NOx pollutant

	Time	Model	Statistics	Meteorological parameters							
				No 1	No 2	No 3	No 4	No 5	No 6	No 7	Local
NOx	Daily	AERMOD (µg/m^3)	Maximum	282.493	369.497	159.912	210.052	242.644	301.776	52.265	103.430
			Median	3.792	3.711	3.757	3.645	3.717	4.084	4.017	2.255
			Minimum	0.375	0.613	0.398	0.500	0.453	0.579	0.523	0.332
			Peak date	02.01.2021	07.02.2021	01.01.2021	03.02.2021	21.05.2021	18.04.2021	01.08.2021	18.09.2021
		CALPUFF (µg/m^3)	Maximum	72.462	103.460	67.041	62.738	67.895	66.295	95.127	166.410
			Median	6.326	6.020	5.025	5.011	5.838	5.886	6.300	7.897
			Minimum	1.437	0.953	0.962	1.202	1.155	1.440	1.049	1.972
			Peak date	05.05.2021	13.12.2021	28.01.2021	18.10.2021	25.04.2021	25.11.2021	05.02.2021	07.05.2021
	Annual	AERMOD (µg/m^3)	Maximum	7.913	12.391	7.977	8.266	8.279	8.312	8.577	9.219
			Median	0.222	0.200	0.214	0.209	0.211	0.198	0.231	0.166
			Minimum	0.044	0.039	0.042	0.043	0.046	0.039	0.030	0.033
		CALPUFF (µg/m^3)	Maximum	19.772	14.636	17.309	19.561	19.445	19.558	21.380	11.457
			Median	0.283	0.262	0.253	0.258	0.263	0.251	0.274	0.398
			Minimum	0.051	0.025	0.033	0.033	0.038	0.032	0.049	0.114

Table 9 Results of simulation models for CO pollutant

	Time	Model	Statistics	Meteorological parameters							
				No 1	No 2	No 3	No 4	No 5	No 6	No 7	Local
CO	Daily	AERMOD (µg/m^3)	Maximum	145.268	190.016	82.235	108.018	124.781	155.187	26.878	53.173
			Median	1.945	1.899	1.923	1.867	1.903	2.092	2.056	1.156
			Minimum	0.192	0.314	0.204	0.256	0.232	0.297	0.268	0.170
			Peak date	02.01.2021	07.02.21	01.01.2021	03.02.2021	21.05.2021	18.04.2021	01.08.2021	18.09.2021
		CALPUFF (µg/m^3)	Maximum	37.250	53.198	34.474	32.129	34.763	34.016	48.927	85.578
			Median	3.286	3.127	2.609	2.596	3.025	3.041	3.275	4.087
			Minimum	0.753	0.502	0.503	0.628	0.606	0.751	0.545	1.041
			Peak date	05.05.2021	13.12.2021	28.01.2021	18.10.2021	25.04.2021	25.11.2021	05.02.2021	07.05.2021
	Annual	AERMOD (µg/m^3)	Maximum	4.047	6.371	4.079	4.227	4.257	4.252	4.389	4.714
			Median	0.113	0.103	0.110	0.107	0.108	0.101	0.119	0.085
			Minimum	0.022	0.020	0.022	0.022	0.024	0.020	0.015	0.017
		CALPUFF (µg/m^3)	Maximum	10.132	7.504	9.831	10.023	9.964	10.023	10.960	5.887
			Median	0.147	0.136	0.139	0.134	0.137	0.130	0.142	0.206
			Minimum	0.027	0.013	0.016	0.017	0.020	0.017	0.026	0.060

models have shown variations in distribution compared to annual models in the inter-model distributions. The annual model distribution of pollutants was mostly in southward regions because the prevailing wind direction is north. The daily maximum and annual average PM_{10} dispersion maps are presented in Figs. 6 and 7.

In this study, especially the NOx and CO daily model results of the AERMOD model, hot spots were observed in Fig. 8 and Fig. 10. The model outputs of these grids showing high concentrations were analysed, and the results showed that these grids had a high concentration some days. At the same time, the regions of hotspot distribution were also similar between the physics options. Surface and upper air, which are the meteorological inputs utilised in the AERMOD model, were analysed recently, and low wind speeds were discovered. CALPUFF model provides better outcomes than the AERMOD model under calm conditions and wind speed because CALPUFF can utilise wind speed data on a more precise scale (Scire et al. 2000; Gulia et al. 2015; Mak et al. 2020). However, the puff model used in the CALPUFF model is more successful in estimating concentrations at low wind speeds than using the Gaussian dispersion model in AERMOD (Holmes and Morawska 2006; Qian and Venkatram 2011; Zeydan and Karademir 2023). Although it has been emphasised that the variations in topography utilised for the AERMOD and CALPUFF models may influence the distribution, in this work, SRTM3 data were used for AERMOD and CORINE data for CALPUFF (Demirarslan et al.

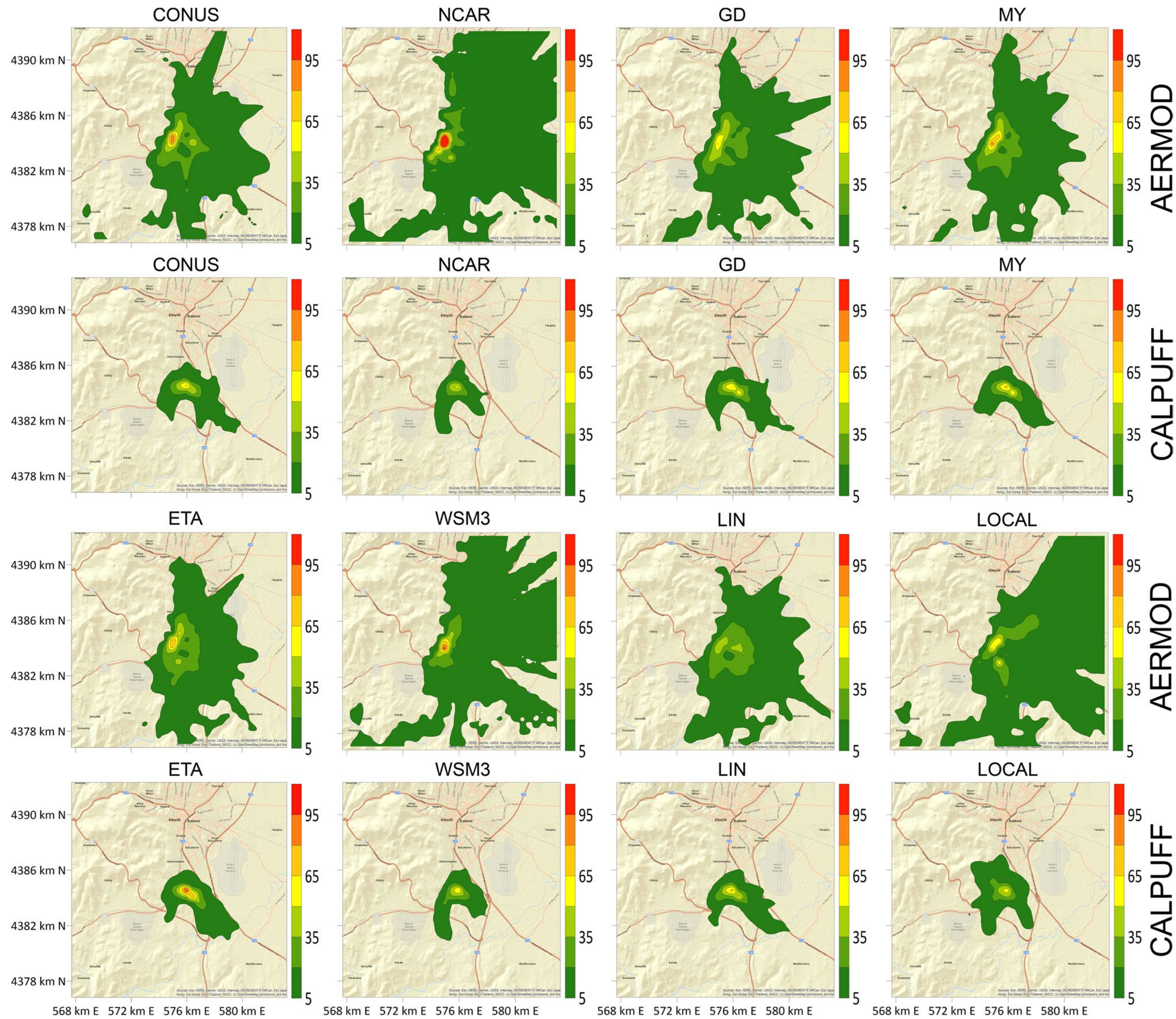

Fig. 6 Dispersion maps of daily maximum PM_{10} levels

2017). Based on the data, hotspot grids are expected to prove effective due to factors such as low wind speed, environmental variables, and model variations. NOx and CO of the daily maximum and annual average dispersion maps are presented in Figs. 8, 9, 10, and 11.

The meteorological inputs were utilised with two different options. Satellite meteorological data GDAS and ERA are validated datasets used for large areas and many studies (Su et al. 2015; Haider et al. 2020; Gunwani et al. 2023). Moreover, these data sets have the advantages of being compatible with various meteorological simulation models, such as WRF and MM5. On the contrary, the distance of local stations to the study area and missing data cause uncertainties in the results. In this study, it is assumed that difficulties such as local station data being far from the operation and missing data being replaced with previous-year data impact the model results. Another part is the effect of the physics used for WRF on the models. The physics models process many different meteorological data units, such as ds083.3 data, which has 35 different meteorological data sets. Air quality dispersion is affected by many variables, such as meteorology and topography, however, the primary causes of dispersion are generally (Verma and Desai 2008; Chen et al. 2015; Bozhkova et al. 2020). The WRF can estimate complicated weather phenomena such as rainfall, hurricanes, and climate change, which are difficult to anticipate. In summary, WRF physics options exhibited similar distribution and results, which may be read as the fact that the meteorological data outputs provided results close to each other.

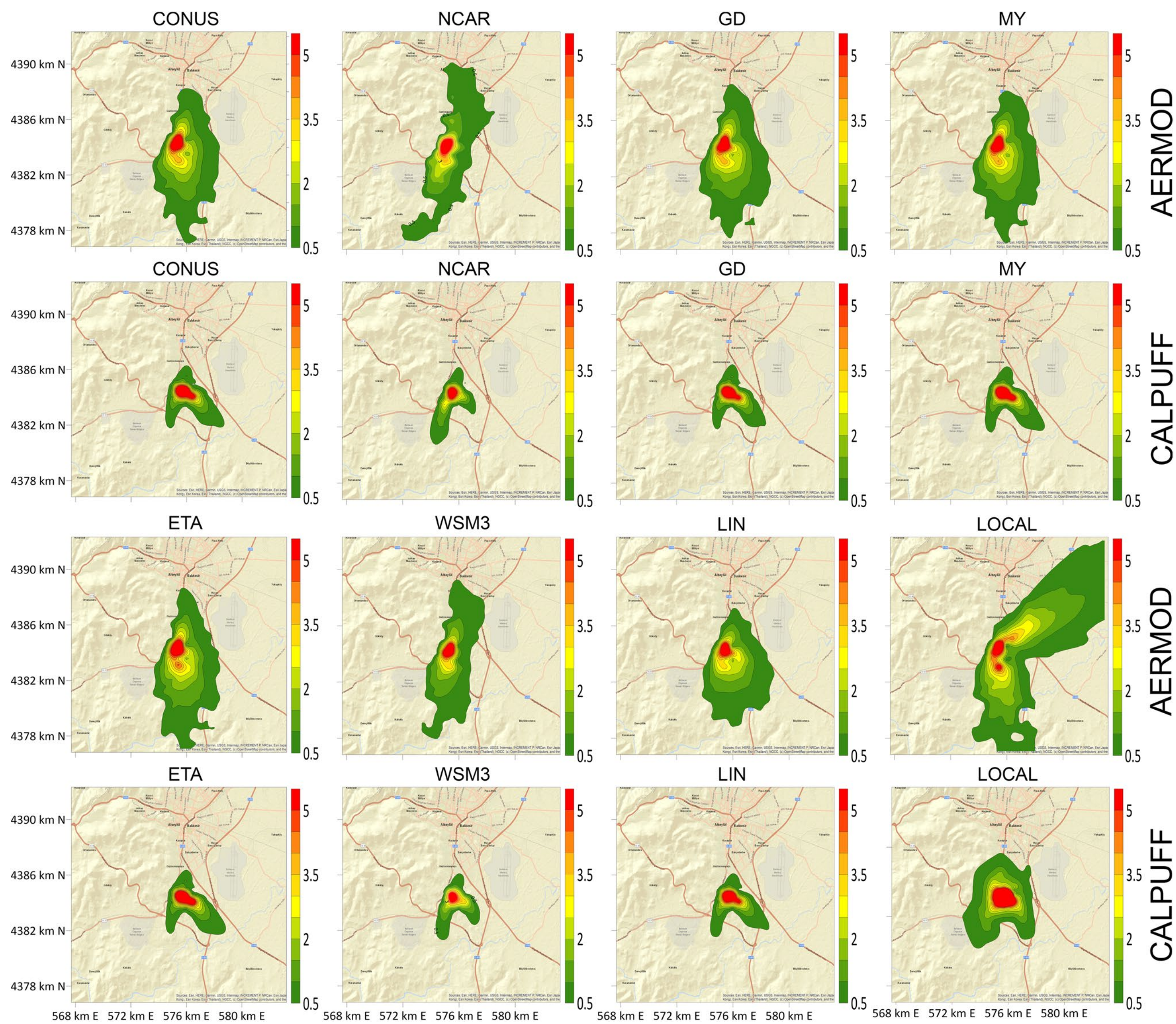

Fig. 7 Dispersion maps of annual average PM_{10} levels

Health risk

In this study, in addition to PM_{10}, NOx, and CO emissions used for air quality dispersion models, along with heavy metal pollutants released from the source, there are 962 receiver points in total, including the receiver points created in 500 m squares in a total area of 15 x 15 km and Balikesir Central Hospital in Fig. 1. For health risk analysis, acute and chronic risk of respiratory cancer was estimated using only PM_{10} data outputs along with heavy metal data from four chimneys in Table 1. The health risk models were only used for exposure to cement factory and did not use background pollutants or other external sources. The model analysis was designed with the respiratory risk scenario defined as lifetime (70 years) by the EPA. The EPA has determined the minimum expected risk for respiratory cancer as one person per million (1 x 10^{-6}) (US EPA 2009; OEHHA 2015).

In this study, while the limit risk specified by the EPA was exceeded at 49 receiver points in the total of all model results, the highest risk value was 3.08 x 10^{-6} people and the limit value was most frequently exceeded in the results estimated using the CALPUFF-LIN model. At the same time, the "NCAR" physics model showed that the maximum cancer risk ratio for AERMOD was 1.77 x 10^{-6}. It was stated that exceeding the noncarcinogen acute and chronic risk limit values determined by the EPA as 1 would pose a risk (US EPA 2009; OEHHA 2015). On examination of the model results, while there was no receiver point exceeding the limit value of acute risk, the maximum risk value of the receiver point was 0.211. The results with the highest

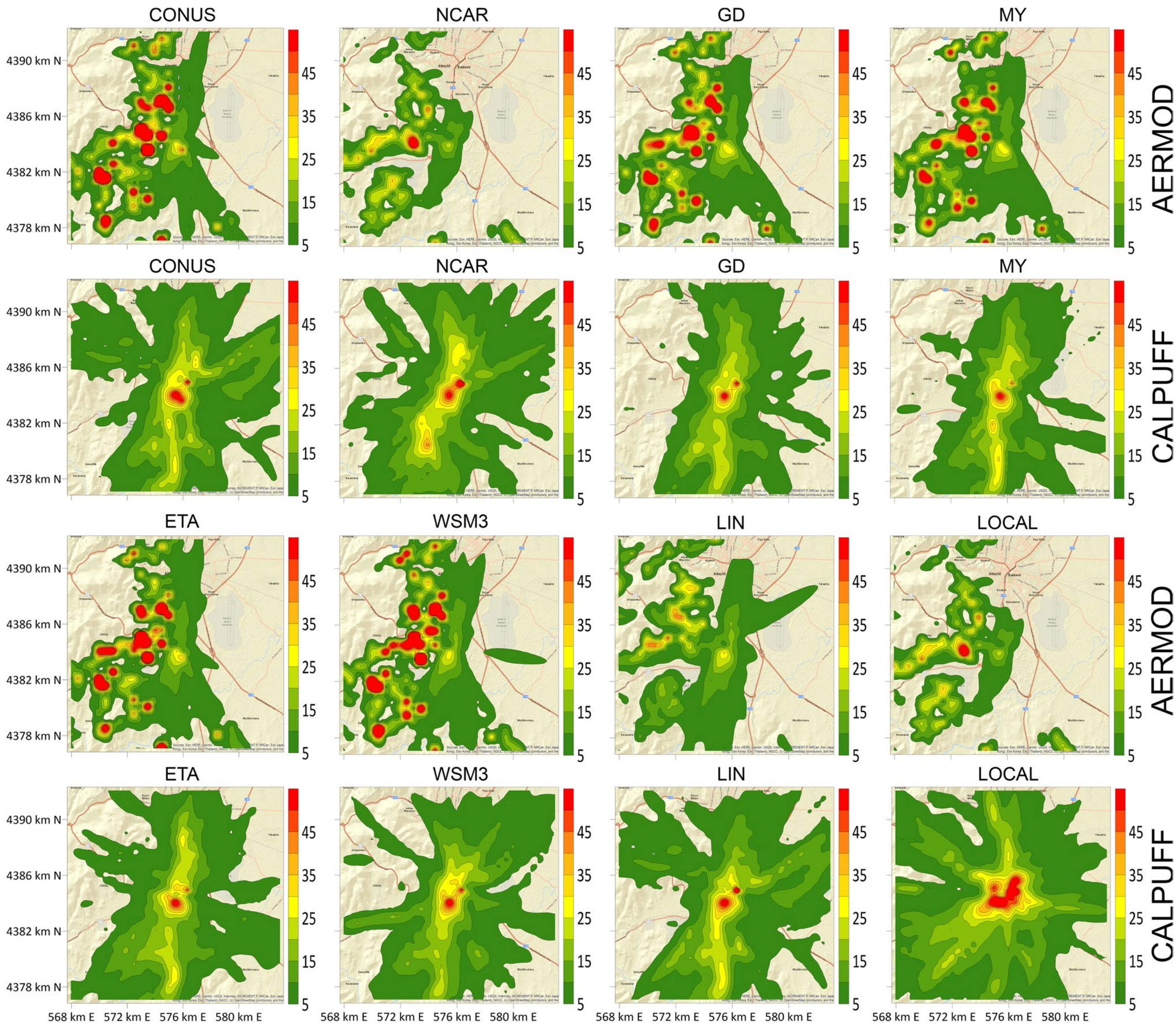

Fig. 8 Dispersion maps of daily maximum NOx levels

acute risk were obtained with the AERMOD model. While the chronic risk limit values were observed to be exceeded at only 5 receiver points in the model results, the highest value of the receiver point was 1.22 with the CALPUFF-LIN model also, which was 500 meters to the south of the central point from the facility. AERMOD-LIN results also have a lower risk rate value of 0.51, which has the highest value in the same position for both models. On examination of the cancer, chronic, and acute risk results in Balikesir Central Hospital which is the closest sensitive point to the facility, only the cancer risk value exceedance was seen with a value of 1.84 x 10^{-6} in the CALPUFF-Local model using the local meteorological data set, while there was no limit exceedance in the acute and chronic risk model results shown on Fig. 12. The cancer value excess of the hospital is highly near to the facility, and local meteorological data also has low wind speed and calm conditions. Therefore, the annual PM_{10} concentration is substantially higher than the other model values.

On the evaluation of the point sources, which compared differences among each other, the highest risk rates were observed predominantly in Stack 1 sources, followed by those discovered in Stack 3, Stack 4, and Stack 2. The findings are believed to be linked to the input sources and influenced by the risk rates derived from the "HARP database" used in this model. When accounting for variations in physics, all dispersion models produce results that closely resemble each other. This connection is particularly evident in assessing PM_{10} concentrations in air quality, which encompass daily and annual measures. Upon

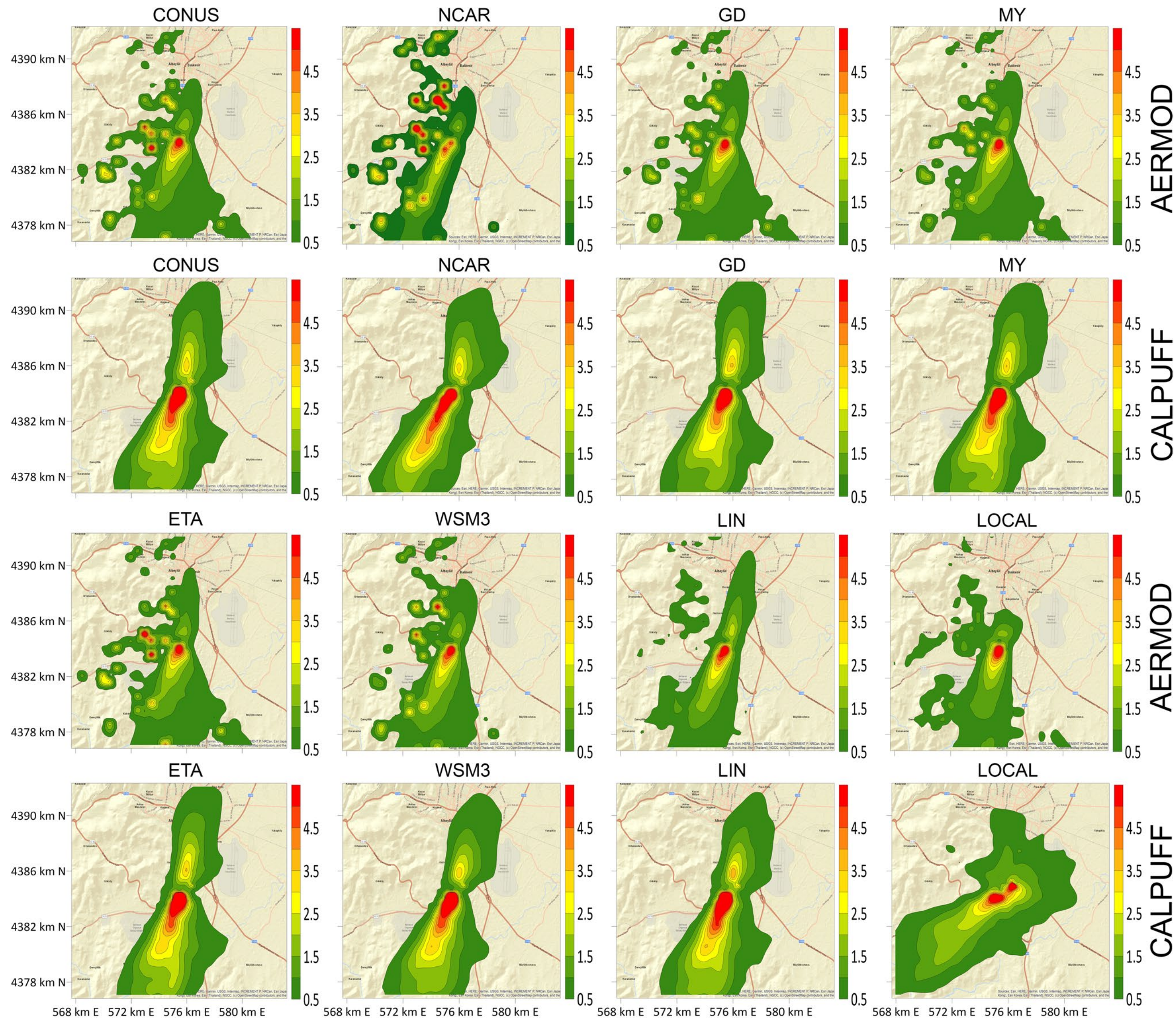

Fig. 9 Dispersion maps of annual average NOx levels

analyzing locations with the highest cancer risk, it was observed that the distributions across the models were consistent. The highest peaks of health risks were identified as 500–1000 meters south of the facility.

In this study, the health risk results for each point measured by the grid points were displayed in a box plot. The line dividing the framed box into two parts is the median value. The top and bottom lines of the framed box plot represent the interquartile range value. The lower and upper lines of the framed box indicate the minimum and maximum health risk values. The outlier data in the box plot has been represented by points. Health risk models are presented in Figs. 13, 14, and 15. In this study, only cancer and acute risks were observed to be exceeded as a result of the evaluations of PM_{10} and heavy metal inputs for emission inputs, respiratory risks, cancer, and acute and chronic lifetime risks.

According to the previous literature, Donoghue and Coffey (2014) examined health risks associated with an aluminium refinery that used a harp model to assess the lifetime exposure level. Also, the risk analysis was conducted at a distance range of 3-5 km. As a consequence, cancer risks were above the limit values. However, acute and chronic risks did not exceed the limit values, and the research also indicated that the PM_{10} pollutant was dominating the acute health risk (Environ Australia 2008). Schuhmacher et al. (2004) estimated the inhalation risk implications of heavy metals from a cement factory, which was the lifetime exposure level. It was found that although cancer risk levels surpassed the limited mean values, the non-cancer risk was within the limit. Parlak et al. (2023) observed that Cr

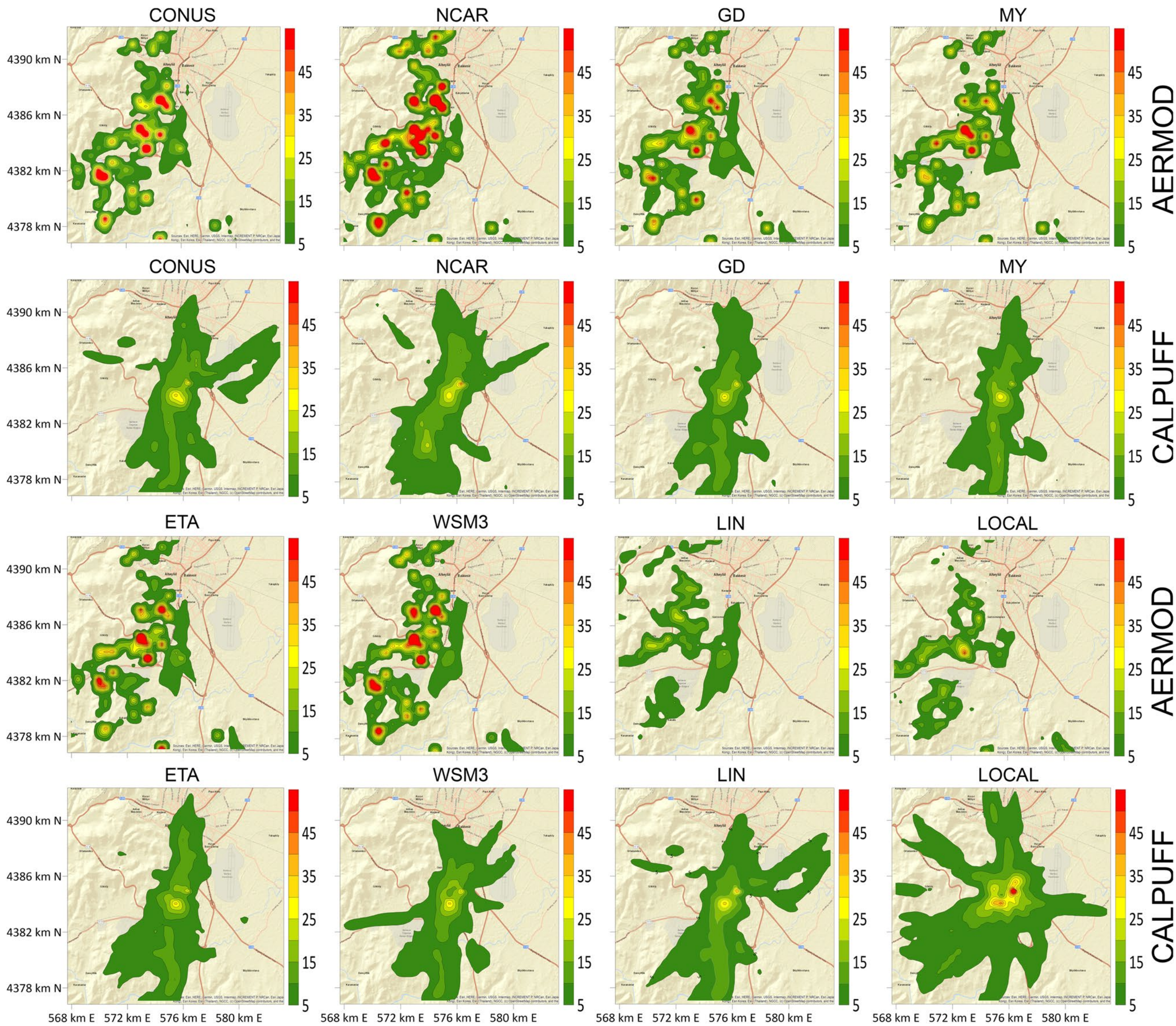

Fig. 10 Dispersion maps of daily maximum CO levels

and Pb pollution from a cement mill in the Canakkale Ezine area, which was close to the Balikesir region, exceeded the acceptable adult limit. Kamaludin et al. (2020) and (Jafari et al. 2023) examined the risks of heavy metal inhalation from the cement industry on workers such that Cr pollutants exceeded the acceptable cancer risk limit values, and the ventilation system, masks, and dust filters were unable to reduce them down to acceptable limit levels.

Summary and conclusions

This study was carried out to analyze the pollution emitted by a cement factory operating in the central region of Balikesir province and to analyze the performance of the models as well as to foresee possible long-term health risks.

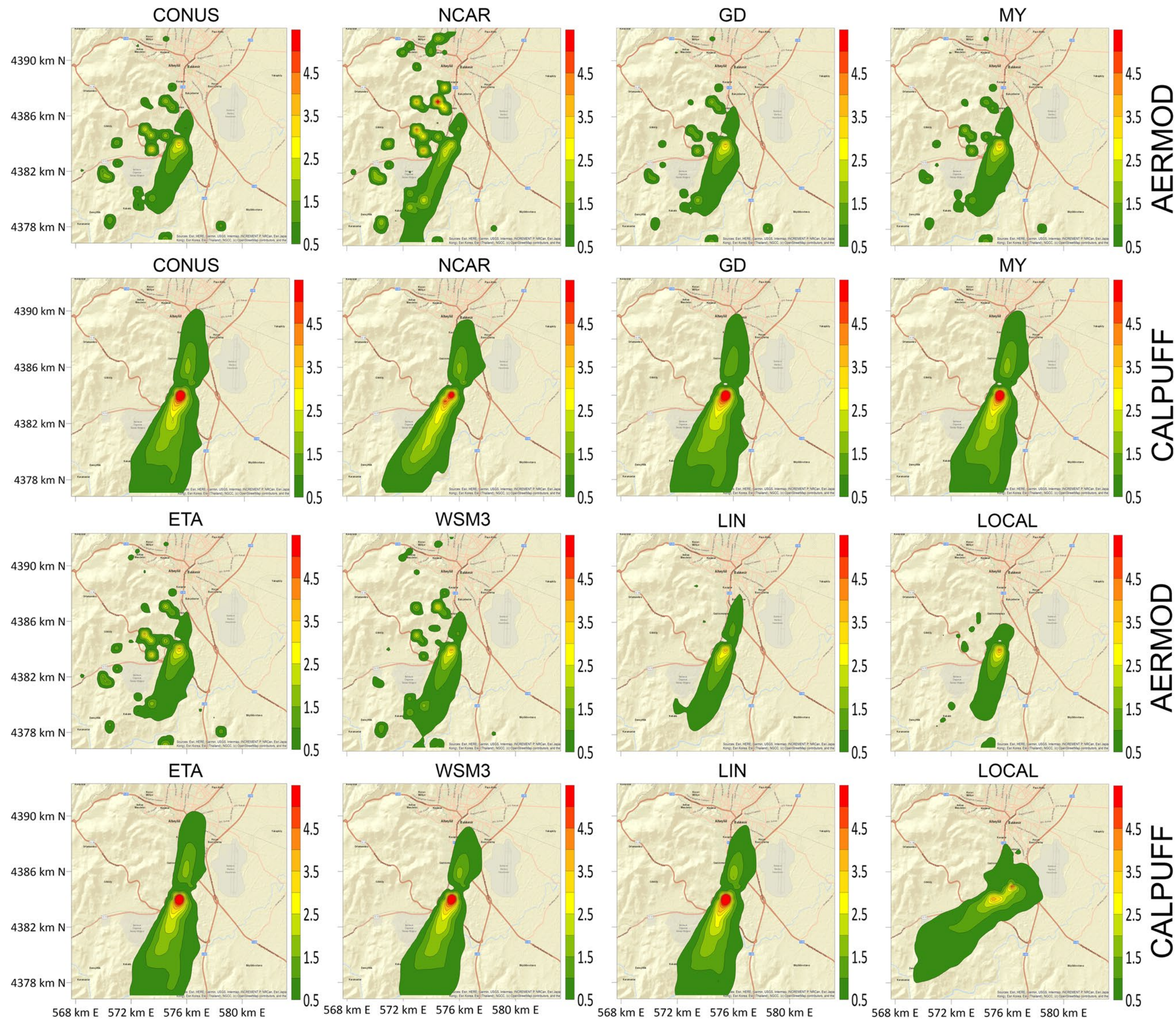

Fig. 11 Dispersion maps of annual average CO levels

Correlation of daily models and AQMS results were accomplished more adequately than the hourly correlation results of both models. The WRF data set utilising GDAS/ERA5 is more suited and dependable for evaluating meteorological simulations than meteorological stations. Among the physics models used for WRF, the best results were achieved with daily No. 3 (GD) and No. 4 (MY) and hourly No. 5 (ETA). Additionally, validation parameters compared to physical models suggest that daily results were more valid than the hourly AQMS results. In this study, it is hard to claim that there is a considerable difference between all physical models. On the other hand, the WRF default physics parameter of No. 1 (CONUS) is compatible and also the other suggested physics No. 2 (NCAR) is suitable for this study. When the air quality dispersion models were compared, while the correlation value of the CALPUFF model was higher, the AERMOD model produced good results as well. Furthermore, the model validation findings of each model are consistent with daily time intervals in pollutant distributions, hence the AERMOD and CALPUFF models are appropriate for this study.

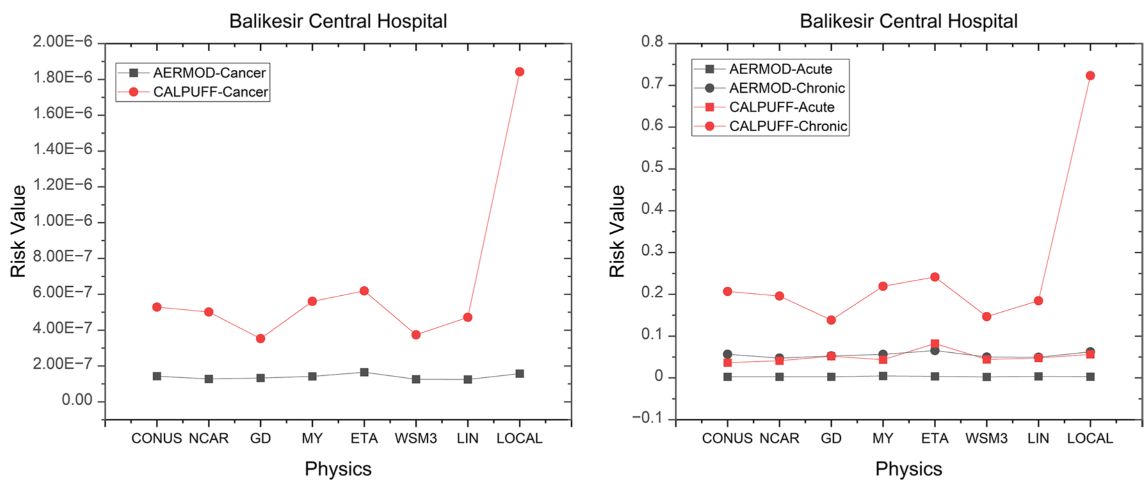

Fig. 12 Risk results of Balikesir Central Hospital

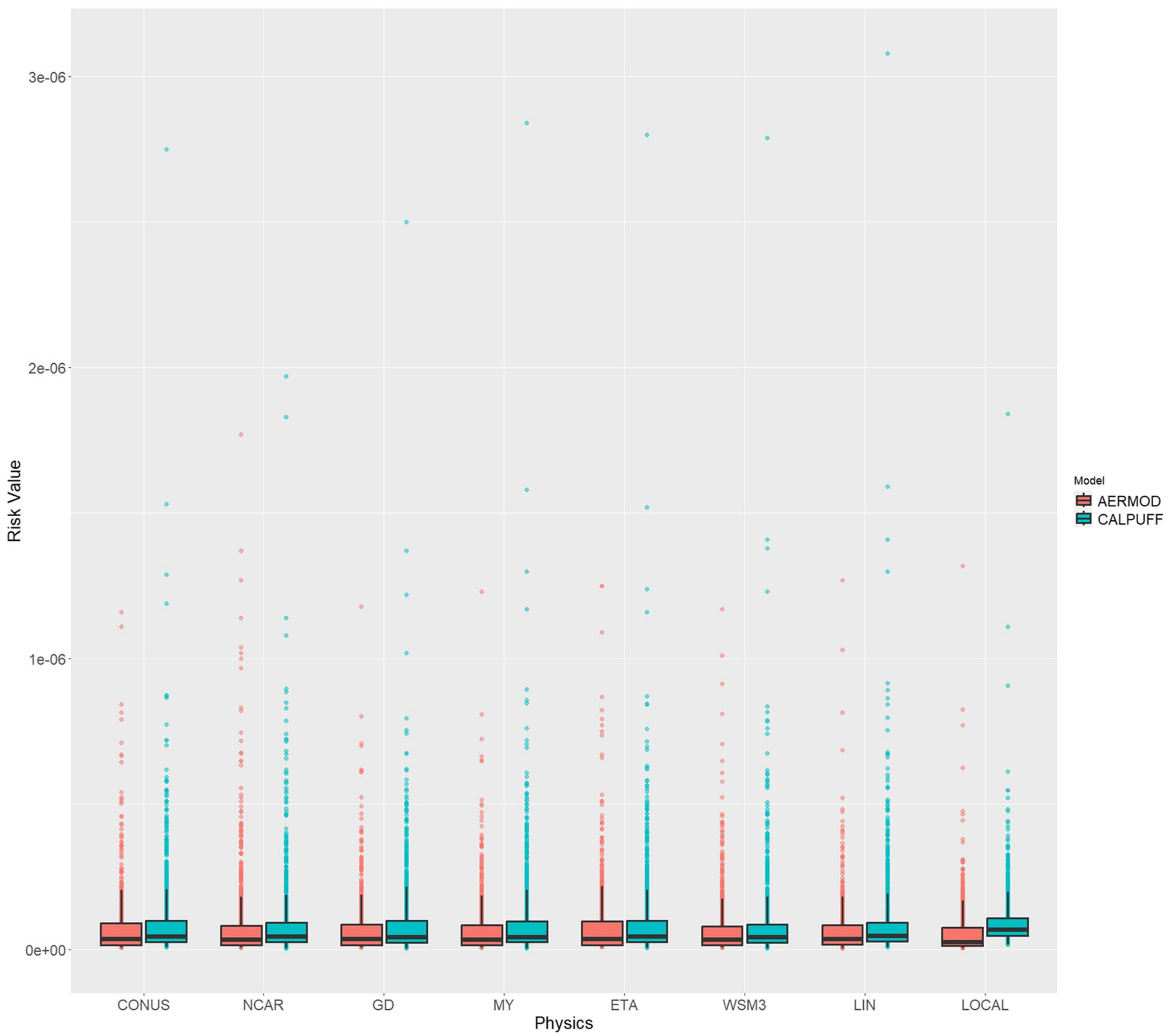

Fig. 13 Cancer risk implications

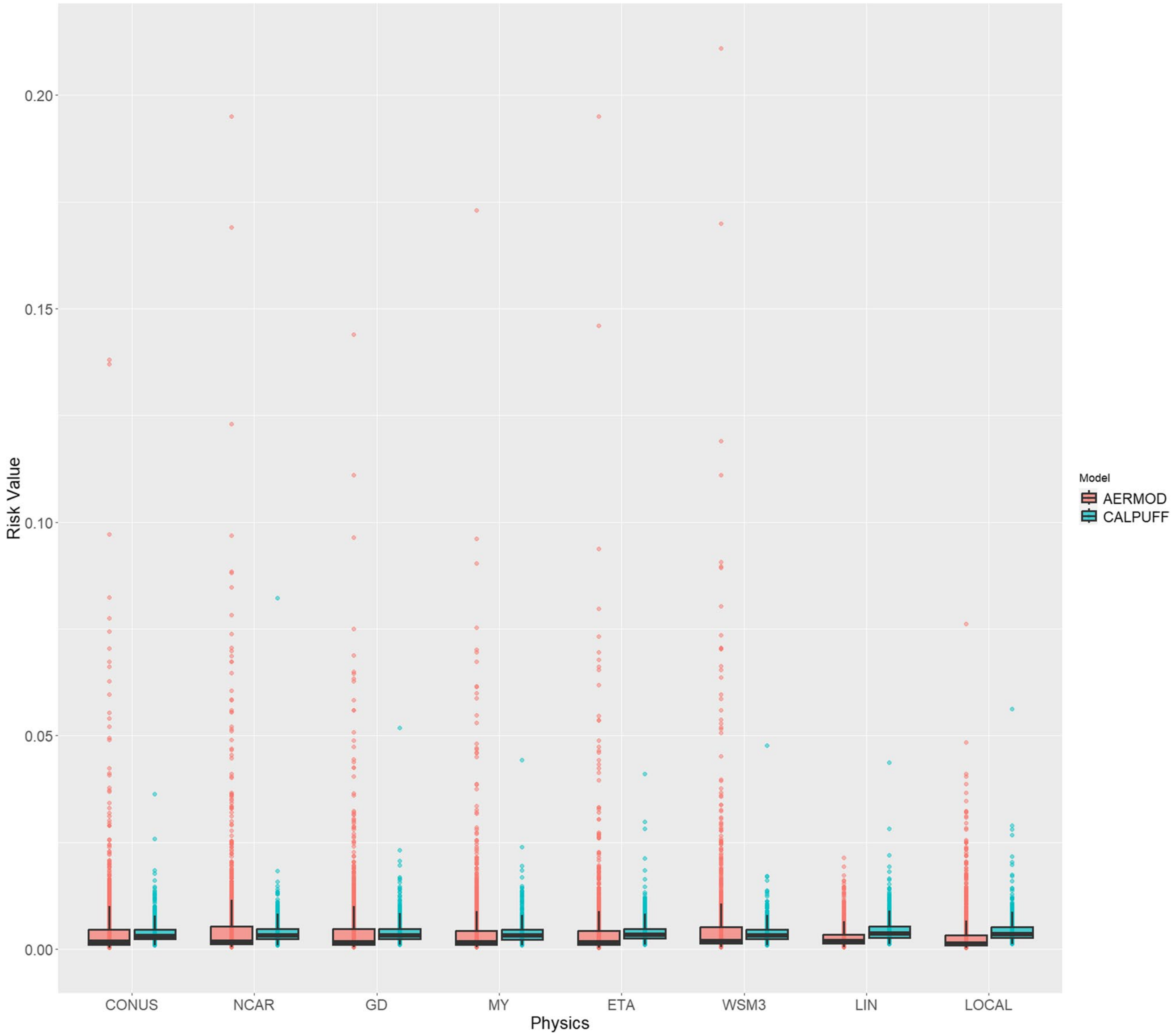

Fig. 14 Acute risk implications

Dispersion model results for PM_{10}, NOx, and CO concentrations reveal that low wind speeds and model features produced differences daily and annually. Further, differences in emission source types exhibited variances in PM_{10}, NOx, and CO distribution maps. While the dispersion was more distributed in the environmental area in the maps created in the hourly period, line and area sources in the near ground had an effect on PM_{10} pollutant distributions. The facility is located in the upwind region. As a result, the distributions for each model showed a southward distribution in long-term. Although the highest concentration values vary depending on the model, pollutant, and period, these were mostly No. 2 (NCAR), No. 6 (WSM3), and local data sets, while the lowest concentration was found particularly in the AERMOD-LIN physic model. While AERMOD obtained the highest concentration levels in daily results, CALPUFF reached higher concentrations in the annual time. The days when the pollutants reached peak concentration were mostly during the winter season.

When the models for health risk analysis were examined, AERMOD and CALPUFF model in health risk results were near to each other. Furthermore, the variation in air quality model findings did not result in a substantial rise in health risk levels. In this study, health risks are negligible for the neighboring settlements in the facility area. Similarly, the Balikesir Central Hospital health risks are negligible for long-term respiratory. Risk exceedances were mostly observed in the southern part of the facility.

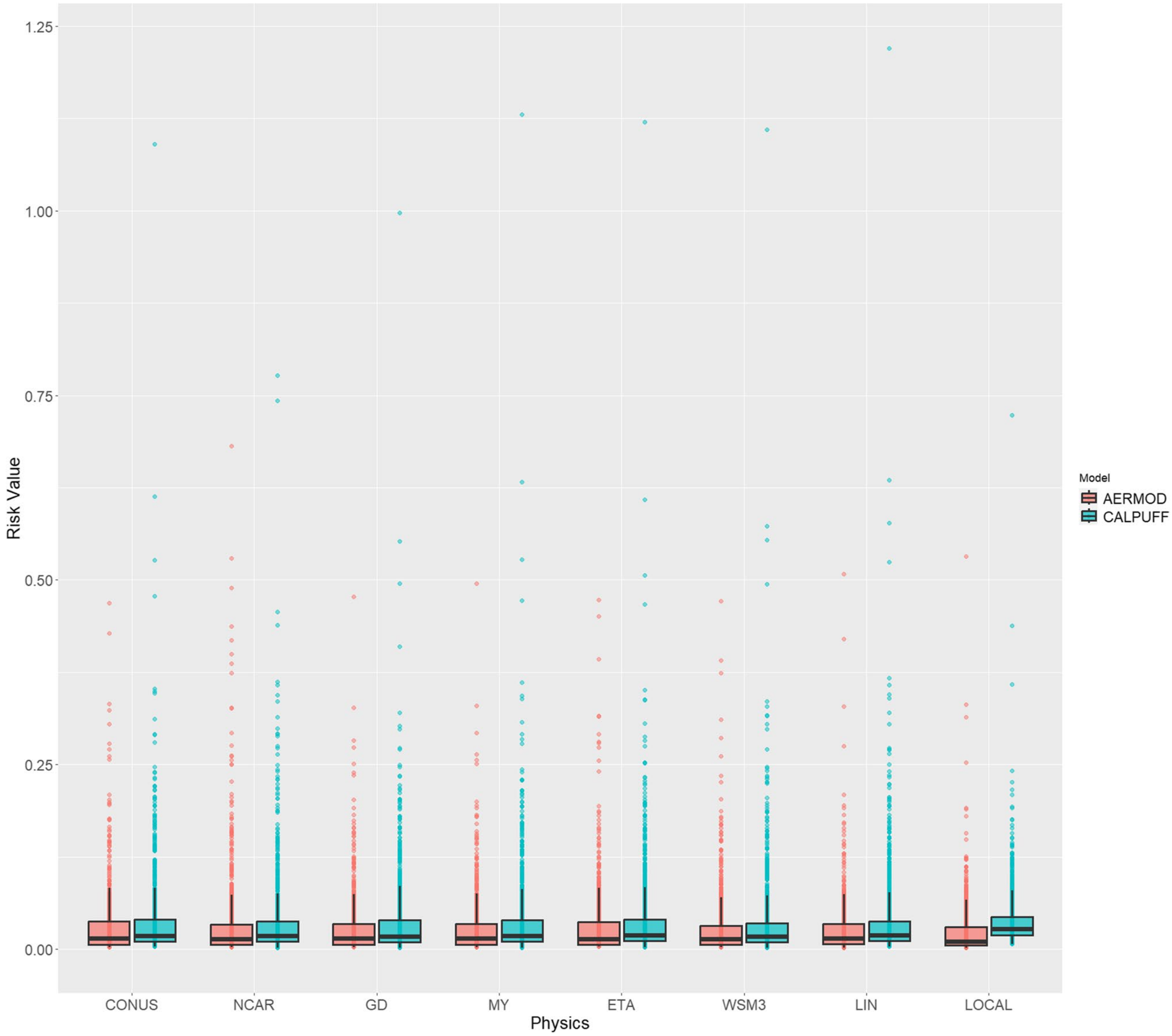

Fig. 15 Chronic risk implications

Acknowledgement This study, the preliminary data were acquired from Omer Mert Bayraktar's master's thesis.

Funding Open access funding provided by the Scientific and Technological Research Council of Türkiye (TÜBİTAK).

Data availability We, as authors, confirm that data will be available on reasonable request.

Declarations

Consent ot publish We, as authors, approved the manuscript for publication.

Competing interests We, as authors, decalre no competing interests

References

Abdul-Wahab S, Sappurd A, Al-Damkhi A (2011) Application of California Puff (CALPUFF) model: a case study for Oman. Clean Techn Environ Policy 13:177–189. https://doi.org/10.1007/s10098-010-0283-7

Adeniran JA, Yusuf RO, Fakinle BS, Sonibare JA (2019) Air quality assessment and modelling of pollutants emission from a major cement plant complex in Nigeria. Atmos Pollut Res 10(1):257–266. https://doi.org/10.1016/j.apr.2018.07.010

Afzali A, Rashid M, Afzali M, Younesi V (2017) Prediction of air pollutants concentrations from multiple sources using AERMOD coupled with WRF prognostic model. J Clean Prod 166:1216–1225. https://doi.org/10.1016/j.jclepro.2017.07.196

Ahrens CD (2015) Meteorology today: an introduction to weather, climate, and the environment. Cengage Learning Canada Inc.

Anderson JO, Thundiyil JG, Stolbach A (2012) Clearing the air: a review of the effects of particulate matter air pollution on human health. J Med Toxicol 8:166–175. https://doi.org/10.1007/s13181-011-0203-1

Arnold S, ApSimon H, Barlow J, Belcher S, Bell M, Boddy J, Britter R, Cheng H, Clark R, Colvile R (2004) Introduction to the DAPPLE air pollution project. Sci Total Environ 332(1-3):139–153. https://doi.org/10.1016/j.scitotenv.2004.04.020

Bayraktar OM (2022) Bir sanayi işletmesinden salınan hava kirleticilerine ait dağılım modellerinin ve olası halk sağlığı etkilerinin incelenmesi. Balıkesir Üniversitesi Fen Bilimleri Enstitüsü https://dspace.balikesir.edu.tr/xmlui/bitstream/handle/20.500.12462/12389/%C3%96mer_Mert_Bayraktar.pdf?sequence=1&isAllowed=y. Accessed 21 Mar 2024

Bayram H, Dörtbudak Z, Fişekçi FE, Kargın M, Bülbül B (2006) "Hava kirliliğinin insan sağlığına etkileri, dünyada, ülkemizde ve bölgemizde hava kirliliği sorunu" paneli ardından. Dicle Tıp Dergisi 33(2):105–112

Bezyk Y, Oshurok D, Dorodnikov M, Sówka I (2021) Evaluation of the CALPUFF model performance for the estimation of the urban ecosystem CO2 flux. Atmos Pollut Res 12(3):260–277. https://doi.org/10.1016/j.apr.2020.12.013

Bildirici ME (2020) The relationship between cement production, mortality rate, air quality, and economic growth for China, India, Brazil, Turkey, and the USA: MScBVAR and MScBGC analysis. Environ Sci Pollut Res 27(2):2248–2263. https://doi.org/10.1007/s11356-019-06586-w

Bishara AJ, Hittner JB (2012) Testing the significance of a correlation with nonnormal data: comparison of Pearson, Spearman, transformation, and resampling approaches. Psychol Methods 17(3):399. https://doi.org/10.1037/a0028087

Boadh R, Satyanarayana A, Krishna TR, Madala S (2016) Sensitivity of PBL schemes of the WRF-ARW model in simulating the boundary layer flow parameters for their application to air pollution dispersion modeling over a tropical station. Atmósfera 29(1):61–81. https://doi.org/10.20937/ATM.2016.29.01.05

Bozhkova VV, Liudchik AM, Umreika SD (2020) Influence of meteorological conditions on urban air pollution. Acta Geograph Silesiana 14(4):5–21

Bukovsky MS, Karoly DJ (2009) Precipitation simulations using WRF as a nested regional climate model. J Appl Meteorol Climatol 48(10):2152–2159. https://doi.org/10.1175/2009JAMC2186.1

Çankaya S, Pekey B (2019) A comparative life cycle assessment for sustainable cement production in Turkey. J Environ Manag 249:109362. https://doi.org/10.1016/j.jenvman.2019.109362

Chang JC (2003) Methodologies for evaluating performance and assessing uncertainty of atmospheric dispersion models. George Mason University

Chang JC, Hanna SR (2004) Air quality model performance evaluation. Meteorog Atmos Phys 87(1-3):167–196

Chen W, Tang H, Zhao H (2015) Diurnal, weekly and monthly spatial variations of air pollutants and air quality of Beijing. Atmos Environ 119:21–34. https://doi.org/10.1016/j.atmosenv.2015.08.040

Ching J, Rotunno R, LeMone M, Martilli A, Kosovic B, Jimenez P, Dudhia J (2014) Convectively induced secondary circulations in fine-grid mesoscale numerical weather prediction models. Mon Weather Rev 142(9):3284–3302. https://doi.org/10.1175/MWR-D-13-00318.1

Chinyama MP (2011) Alternative fuels in cement manufacturing. Alternative Fuel 262-284. https://doi.org/10.5772/22319

Cipriani G, Danti S, Carlesi C, Borin G (2018) Danger in the air: air pollution and cognitive dysfunction. Am J Alzheimers Dis Other Dement 33(6):333–341. https://doi.org/10.1177/1533317518777859

Cui H, Yao R, Xu X, Xin C, Yang J (2011) A tracer experiment study to evaluate the CALPUFF real time application in a near-field complex terrain setting. Atmos Environ 45(39):7525–7532. https://doi.org/10.1016/j.atmosenv.2011.08.041

Davis C, Wang W, Chen SS, Chen Y, Corbosiero K, DeMaria M, Dudhia J, Holland G, Klemp J, Michalakes J (2008) Prediction of landfalling hurricanes with the advanced hurricane WRF model. Mon Weather Rev 136(6):1990–2005. https://doi.org/10.1175/2007MWR2085.1

De Melo AMV, Santos JM, Mavroidis I, Junior NCR (2012) Modelling of odour dispersion around a pig farm building complex using AERMOD and CALPUFF. Comparison with wind tunnel results. Build Environ 56:8–20. https://doi.org/10.1016/j.buildenv.2012.02.017

Demirarslan KO, Çetin Doğruparmak Ş, Karademir A (2017) Evaluation of three pollutant dispersion models for the environmental assessment of a district in Kocaeli, Turkey. Glob NEST Journal 19(1):37–48. https://doi.org/10.30955/GNJ.001901

Dianat M, Radmanesh E, Badavi M, Goudarzi G, Mard SA (2016) The effects of PM_{10} on electrocardiogram parameters, blood pressure and oxidative stress in healthy rats: the protective effects of vanillic acid. Environ Sci Pollut Res 23:19551–19560. https://doi.org/10.1007/s11356-016-7168-1

Donoghue AM, Coffey PS (2014) Health risk assessments for alumina refineries. Journal of Occupational and Environmental Medicine 56(5):S18-S22. https://doi.org/10.1097/JOM.0000000000000011

Dresser AL, Huizer RD (2011) CALPUFF and AERMOD model validation study in the near field: Martins Creek revisited. J Air Waste Manage Assoc 61(6):647–659. https://doi.org/10.3155/1047-3289.61.6.647

Duzenli E, Yucel I, Pilatin H, Yilmaz MT (2021) Evaluating the performance of a WRF initial and physics ensemble over Eastern Black Sea and Mediterranean regions in Turkey. Atmos Res 248:105184. https://doi.org/10.1016/j.atmosres.2020.105184

Efstathiou G, Zoumakis N, Melas D, Lolis C, Kassomenos P (2013) Sensitivity of WRF to boundary layer parameterizations in simulating a heavy rainfall event using different microphysical schemes. Effect on large-scale processes. Atmos Res 132:125–143. https://doi.org/10.1016/j.atmosres.2013.05.004

Report EIA (2014) Cement Plant EIA Report. In: Provincial Environmental Agency in Balikesir. (Ministry of Environmental and Urbanization, Ankara, Issue

Eltahan M, Magooda M (2018) Sensitivity of WRF microphysics schemes: Case study of simulating a severe rainfall over Egypt. J Phys Conf Ser 1039(1). https://doi.org/10.1088/1742-6596/1039/1/012024

Emert AD, Griffis-Kyle K, Portillo-Quintero C, Smith PN (2024) USEPA CALPUFF validation and dispersion modeling of beef cattle feedlot PM10 and PM2.5 emissions factors. Atmos Environ 316:120189. https://doi.org/10.1016/j.atmosenv.2023.120189

Environ Australia (2008) Screening Health Risk Assessment of Particulate Emissions From Alcoa's Pinjarra Refinery Residue Disposal Area. https://www.alcoa.com/australia/en/pdf/HRA_Pinjarra_Dust_21_August_08.pdf. Accessed 21 Mar 2024

Eslamidoost Z, Arabzadeh M, Oskoie V, Dehghani S, Samaei MR, Hashemi H, Baghapour MA (2022) Dispersion of NO2 pollutant in a gas refinery with AERMOD model: A case study in the Middle East. J Air Pollut Health. https://doi.org/10.18502/japh.v7i3.10544

Eslamidoost Z, Samaei MR, Hashemi H, Baghapour MA, Arabzadeh M, Dehghani S, Rajabi S (2023) Assessment of air quality using AERMOD modeling: a case study in the Middle East. Environ Monit Assess 195(11):1272. https://doi.org/10.1007/s10661-023-11879-2

Evans JP, Ekström M, Ji F (2012) Evaluating the performance of a WRF physics ensemble over South-East Australia. Clim Dyn 39:1241–1258. https://doi.org/10.1007/s00382-011-1244-5

Fenger J (2009) Air pollution in the last 50 years–From local to global. Atmos Environ 43(1):13–22. https://doi.org/10.1016/j.atmosenv.2008.09.061

FLAG (2010) Federal Land Managers' Air Quality Related Values Work Group (FLAG). Phase I Report. https://www.fws.gov/guidance/sites/guidance/files/documents/FLAG%20Air%20Quality%20Phase%201%20report.pdf. Accessed 21 Mar 2024

Fu F, Purvis-Roberts KL, Williams B (2020) Impact of the COVID-19 pandemic lockdown on air pollution in 20 major cities around the world. Atmosphere 11(11):1189. https://doi.org/10.3390/atmos11111189

Fustos-Toribio I, Manque-Roa N, Vásquez Antipan D, Hermosilla Sotomayor M, Letelier Gonzalez V (2022) Rainfall-induced landslide early warning system based on corrected mesoscale numerical models: an application for the southern Andes. Nat Hazards Earth Syst Sci 22(6):2169–2183. https://doi.org/10.5194/nhess-22-2169-2022

Galvez-Martos J-L, Schoenberger H (2014) An analysis of the use of life cycle assessment for waste co-incineration in cement kilns. Resour Conserv Recycl 86:118–131. https://doi.org/10.1016/j.resconrec.2014.02.009

Gbode IE, Dudhia J, Ogunjobi KO, Ajayi VO (2019) Sensitivity of different physics schemes in the WRF model during a West African monsoon regime. Theor Appl Climatol 136:733–751. https://doi.org/10.1007/s00704-018-2538-x

Ghannam K, El-Fadel M (2013) Emissions characterization and regulatory compliance at an industrial complex: an integrated MM5/CALPUFF approach. Atmos Environ 69:156–169. https://doi.org/10.1016/j.atmosenv.2012.12.022

Goldberg M, Cheng H, Villeneuve PJ (2008) A systematic review of the relation between long-term exposure to ambient air pollution and chronic diseases. Rev Environ Health 23(4):243–298. https://doi.org/10.1515/reveh.2008.23.4.243

Guan W-J, Zheng X-Y, Chung KF, Zhong N-S (2016) Impact of air pollution on the burden of chronic respiratory diseases in China: time for urgent action. Lancet 388(10054):1939–1951. https://doi.org/10.1016/S0140-6736(16)31597-5

Guarnieri M, Balmes JR (2014) Outdoor air pollution and asthma. Lancet 383(9928):1581–1592. https://doi.org/10.1016/S0140-6736(14)60617-6

Güğül GN, Başbilen GD, Baker DK (2023) Techno-economic analysis for wind energy projects: A comparative study with three wind turbines based on real-site data. Turkish J Electr Power Energy Syst 3(3):115–124. https://doi.org/10.5152/tepes.2023.23019

Gulia S, Kumar A, Khare M (2015) Performance evaluation of CALPUFF and AERMOD dispersion models for air quality assessment of an industrial complex. J Sci Ind Res 74:302–307

Gulliver J, Briggs D (2011) STEMS-Air: A simple GIS-based air pollution dispersion model for city-wide exposure assessment. Sci Total Environ 409(12):2419–2429. https://doi.org/10.1016/j.scitotenv.2011.03.004

Gunwani P, Govardhan G, Jena C, Yadav P, Kulkarni S, Debnath S, Pawar PV, Khare M, Kaginalkar A, Kumar R (2023) Sensitivity of WRF/Chem simulated PM2.5 to initial/boundary conditions and planetary boundary layer parameterization schemes over the Indo-Gangetic Plain. Environ Monit Assess 195(5):560. https://doi.org/10.1007/s10661-023-10987-3

Haider MR, Peña M, Lazin R, Khadim FK, Yang M, Dokou Z, Nikolopoulos E, Wang G, Anagnostou E (2020) Enabling water and agriculture management in the upper Blue Nile basin through numerical seasonal forecasts and high-resolution sectoral models. In: 44th NOAA Annual Climate Diagnostics and Prediction Workshop. NOAA, Durham, NC, pp 154–159

Hanna S, Chang J (2012) Acceptance criteria for urban dispersion model evaluation. Meteorog Atmos Phys 116:133–146. https://doi.org/10.1007/s00703-011-0177-1

Hanna SR, Egan BA, Purdum J, Wagler J (2001) Evaluation of the ADMS, AERMOD, and ISC3 dispersion models with the OPTEX, Duke Forest, Kincaid, Indianapolis and Lovett field datasets. Int J Environ Pollut 16(1-6):301–314. https://doi.org/10.1504/IJEP.2001.000626

Harnett B, Hawes T, Allen T (2008) Technical Issues Related to Use of the CALPUFF Modeling System for Near-field Applications. Research Triangle Park

Hendriks CA, Worrell E, De Jager D, Blok K, Riemer P (1998) Emission reduction of greenhouse gases from the cement industry. In: Greenhouse Gas Control Technologies Conference, pp 939–944

Hersbach H, Bell B, Berrisford P, Hirahara S, Horányi A, Muñoz-Sabater J, Nicolas J, Peubey C, Radu R, Schepers D (2020) The ERA5 global reanalysis. Q J R Meteorol Soc 146(730):1999–2049. https://doi.org/10.1002/qj.3803

Hines KM, Bromwich DH (2008) Development and testing of Polar WRF model. Part I: Greenland ice sheet meteorology. Mon Weather Rev 136(6):1971–1989. https://doi.org/10.1175/2007MWR2112.1

Hoinaski L, Franco D, de Melo LH (2017) An analysis of error propagation in AERMOD lateral dispersion using Round Hill II and Uttenweiller experiments in reduced averaging times. Environ Technol 38(5):639–651. https://doi.org/10.1080/09593330.2016.1205672

Holmes NS, Morawska L (2006) A review of dispersion modelling and its application to the dispersion of particles: An overview of different dispersion models available. Atmos Environ 40(30):5902–5928. https://doi.org/10.1016/j.atmosenv.2006.06.003

Holnicki P, Kałuszko A, Trapp W (2016) An urban scale application and validation of the CALPUFF model. Atmos Pollut Res 7(3):393–402. https://doi.org/10.1016/j.apr.2015.10.016

Ilten N, Selici AT (2008) Investigating the impacts of some meteorological parameters on air pollution in Balikesir, Turkey. Environ Monit Assess 140:267–277. https://doi.org/10.1007/s10661-007-9865-1

IPCC (2007) Climate Change 2007: The Physical Science Basis. In: Contribution of Working Group I to the Fourth Assessment Report of the Intergovernmental Panel on Climate Change (IPCC), United Kingdom and New York

Irwin JS (2014) A suggested method for dispersion model evaluation. J Air Waste Manage Assoc 64(3):255–264. https://doi.org/10.1080/10962247.2013.833147

Jafari A, Asadyari S, Moutab Sahihazar Z, Hajaghazadeh M (2023) Monte Carlo-based probabilistic risk assessment for cement workers exposed to heavy metals in cement dust.

Environ Geochem Health 45:5961–5979. https://doi.org/10.1007/s10653-023-01611-x

Jittra N, Pinthong N, Thepanondh S (2015) Performance evaluation of AERMOD and CALPUFF air dispersion models in industrial complex area. Air, Soil and Water Research 8:87–95. https://doi.org/10.4137/ASWR.S32781

Jung S-H, Im E-S, Han S-O (2012) The effect of topography and sea surface temperature on heavy snowfall in the Yeongdong region: A case study with high resolution WRF simulation. Asia-Pac J Atmos Sci 48:259–273. https://doi.org/10.1007/s13143-012-0026-2

Kamaludin NH, Jalaludin J, Tamrin SBM, Akim AM, Martiana T, Widajati N (2020) Exposure to silica, arsenic, and chromium (VI) in cement workers: a probability health risk assessment. Aerosol Air Qual Res 20:2347–2370. https://doi.org/10.4209/aaqr.2019.12.0656

Kampa M, Castanas E (2008) Human health effects of air pollution. Environ Pollut 151(2):362–367. https://doi.org/10.1016/j.envpol.2007.06.012

Kesarkar AP, Dalvi M, Kaginalkar A, Ojha A (2007) Coupling of the Weather Research and Forecasting Model with AERMOD for pollutant dispersion modeling. A case study for PM10 dispersion over Pune, India. Atmos Environ 41(9):1976–1988. https://doi.org/10.1016/j.atmosenv.2006.10.042

Kinney PL (2018) Interactions of climate change, air pollution, and human health. Curr Environ Health Rep 5:179–186. https://doi.org/10.1007/s40572-018-0188-x

Lara-Fanego V, Ruiz-Arias J, Pozo-Vázquez D, Santos-Alamillos F, Tovar-Pescador J (2012) Evaluation of the WRF model solar irradiance forecasts in Andalusia (southern Spain). Sol Energy 86(8):2200–2217. https://doi.org/10.1016/j.solener.2011.02.014

Leone V, Cervone G, Iovino P (2016) Impact assessment of PM 10 cement plants emissions on urban air quality using the SCIPUFF dispersion model. Environ Monit Assess 188:1–12. https://doi.org/10.1007/s10661-016-5519-5

Li X, Yang Y, Xu X, Xu C, Hong J (2016) Air pollution from polycyclic aromatic hydrocarbons generated by human activities and their health effects in China. J Clean Prod 112:1360–1367. https://doi.org/10.1016/j.jclepro.2015.05.077

Li Z, Hu Y, Chen L, Wang L, Fu D, Ma H, Fan L, An C, Liu A (2018) Emission factors of NOx, SO2, and PM for bathing, heating, power generation, coking, and cement industries in Shanxi, China: Based on field measurement. Aerosol Air Qual Res 18(12):3115–3127. https://doi.org/10.4209/aaqr.2018.08.0282

Lo JCF, Yang ZL, Pielke RA Sr (2008) Assessment of three dynamical climate downscaling methods using the Weather Research and Forecasting (WRF) model. J Geophys Res 113(D09112). https://doi.org/10.1029/2007JD009216

MacIntosh DL, Stewart JH, Myatt TA, Sabato JE, Flowers GC, Brown KW, Hlinka DJ, Sullivan DA (2010) Use of CALPUFF for exposure assessment in a near-field, complex terrain setting. Atmos Environ 44(2):262–270. https://doi.org/10.1016/j.atmosenv.2009.09.023

Mahala BK, Mohanty PK, Nayak BK (2015) Impact of microphysics schemes in the simulation of cyclone phailinusing WRF model. Procedia Eng 116:655–662. https://doi.org/10.1016/j.proeng.2015.08.342

Mak J, Taylor C, Fillingham M, McEvoy J (2020) Comparison of the performance of AERMOD and CALPUFF dispersion model outputs to monitored data. In: Mensink C, Gong W, Hakami A (eds) Air pollution modeling and its application XXVI 36. Springer International Publishing, Cham, pp 357–362. https://doi.org/10.1007/978-3-030-22055-6_57

Maleki H, Sorooshian A, Goudarzi G, Nikfal A, Baneshi MM (2016) Temporal profile of PM10 and associated health effects in one of the most polluted cities of the world (Ahvaz, Iran) between 2009 and 2014. Aeolian Res 22:135–140. https://doi.org/10.1016/j.aeolia.2016.08.006

Martinez JA, Arias PA, Castro C, Chang HI, Ochoa-Moya CA (2019) Sea surface temperature-related response of precipitation in northern South America according to a WRF multi-decadal simulation. Int J Climatol 39(4):2136–2155. https://doi.org/10.1002/joc.5940

Mayer H (1999) Air pollution in cities. Atmos Environ 33(24-25):4029–4037. https://doi.org/10.1016/S1352-2310(99)00144-2

Michalakes J, Dudhia J, Gill D, Henderson T, Klemp J, Skamarock W, Wang W (2005) The weather research and forecast model: software architecture and performance. In: Use of High Performance Computing in Meteorology Proceedings of the Eleventh ECMWF Workshop, pp 156–168. https://doi.org/10.1142/9789812701831_0012

Miller SA, Moore FC (2020) Climate and health damages from global concrete production. Nat Clim Chang 10(5):439–443. https://doi.org/10.1038/s41558-020-0733-0

MOEUCC (2020) Balıkesir ili temiz hava eylem planı. https://webdosya.csb.gov.tr/db/balikesir/menu/thep-son-26_20200310014921.pdf. Accessed 10 Oct 2023

Molinari J, Dudek M (1992) Parameterization of convective precipitation in mesoscale numerical models: A critical review. Mon Weather Rev 120(2):326–344. https://doi.org/10.1175/1520-0493(1992)120<0326:POCPIM>2.0.CO;2

Morrison H, Milbrandt J (2011) Comparison of two-moment bulk microphysics schemes in idealized supercell thunderstorm simulations. Mon Weather Rev 139(4):1103–1130. https://doi.org/10.1175/2010MWR3433.1

Mosca S, Benedetti P, Guerriero E, Rotatori M (2014) Assessment of nitrous oxide emission from cement plants: Real data measured with both Fourier transform infrared and nondispersive infrared techniques. J Air Waste Manag Assoc 64(11):1270–1278. https://doi.org/10.1080/10962247.2014.936986

Mueller SF, Bailey EM, Kelsoe JJ (2004) Geographic Sensitivity of Fine Particle Mass to Emissions of SO2 and NOx. Environ Sci Technol 38(2):570–580. https://doi.org/10.1021/es021016n

Muñoz-Sabater J, Dutra E, Agustí-Panareda A, Albergel C, Arduini G, Balsamo G, Boussetta S, Choulga M, Harrigan S, Hersbach H (2021) ERA5-Land: A state-of-the-art global reanalysis dataset for land applications. Earth Syst Sci Data 13(9):4349–4383. https://doi.org/10.5194/essd-13-4349-2021

Mutlu A (2019) Balıkesir şehir merkezinde trafik kaynaklı hava kirliliği seviyelerinin analizi. Balıkesir Üniversitesi Fen Bilimleri Enstitüsü Dergisi 21(1):152–168. https://doi.org/10.25092/baunfbed.532605

Mutlu A (2020) Air quality impact of particulate matter (PM10) releases from an industrial source. Environ Monit Assess 192:1–17. https://doi.org/10.1007/s10661-020-08508-7

Mutlu A, Bayraktar OM (2021) Urban scale air quality analysis due to coal-based residential heating. Air Qual Atmos Health 14:1487–1503. https://doi.org/10.1007/s11869-021-01063-1

NCAR (2017) WRF-ARW V3: User's Guide. http://www2.mmm.ucar.edu/wrf/users/docs/user_guide_V3/user_guide_V3.9/ARWUsersGuideV3.9.pdf. Accessed 21 Mar 2024

NCEP (2015) NCEP GDAS/FNL 0.25 degree global tropospheric analyses and forecast grids. https://doi.org/10.5065/D65Q4T4Z

OEHHA (2009) Technical Support Document for Cancer Potency Factors: Methodologies for derivation, listing of available values, and adjustments to allow for early life stage exposures. https://oehha.ca.gov/media/downloads/crnr/tsdcancerpotency.pdf. Accessed 21 Feb 2024

OEHHA (2015) Risk Assessment Guidelines Guidance Manual for Preparation of Health Risk Assessments. https://oehha.ca.gov/

media/downloads/crnr/2015guidancemanual.pdf. Accessed 21 Feb 2024

Özen C, Dinç U, Deniz A, Karan H (2021) Wind power generation forecast by coupling numerical weather prediction model and gradient boosting machines in Yahyalı wind power plant. Wind Eng 45(5):1256–1272. https://doi.org/10.1177/0309524X20972115

Parlak M, Everest T, Tunçay T (2023) Spatial distribution of heavy metals in soils around cement factory and health risk assessment: a case study of Canakkale-Ezine (NW Turkey). Environ Geochem Health 45:5163–5179. https://doi.org/10.1007/s10653-023-01578-9

Patel P, Ghosh S, Kaginalkar A, Islam S, Karmakar S (2019) Performance evaluation of WRF for extreme flood forecasts in a coastal urban environment. Atmos Res 223:39–48. https://doi.org/10.1016/j.atmosres.2019.03.005

Qian W, Venkatram A (2011) Performance of steady-state dispersion models under low wind-speed conditions. Bound-Layer Meteorol 138:475–491. https://doi.org/10.1007/s10546-010-9565-1

Raffetti E, Treccani M, Donato F (2019) Cement plant emissions and health effects in the general population: a systematic review. Chemosphere 218:211–222. https://doi.org/10.1016/j.chemosphere.2018.11.088

Ramanathan V, Feng Y (2009) Air pollution, greenhouse gases and climate change: Global and regional perspectives. Atmos Environ 43(1):37–50. https://doi.org/10.1016/j.atmosenv.2008.09.063

Rao S, Klimont Z, Smith SJ, Van Dingenen R, Dentener F, Bouwman L, Riahi K, Amann M, Bodirsky BL, van Vuuren DP (2017) Future air pollution in the Shared Socio-economic Pathways. Glob Environ Chang 42:346–358. https://doi.org/10.1016/j.gloenvcha.2016.05.012

Rashidifard M, Rashidi Y, Amiri M (2018) Comparison of AERMOD and CALPUFF models in atmospheric pollutant diffusion modeling (Case Study: Steel Factory). J Environ Sci Stud 2(4):589–597

Rauf AU, Mallongi A, Daud A, Hatta M, Al-Madhoun W, Amiruddin R, Rahman SA, Wahyu A, Astuti RDP (2021) Community health risk assessment of total suspended particulates near a cement plant in Maros Regency. Indonesia J Health Pollut 11(30):1–13. https://doi.org/10.5696/2156-9614-11.30.210616

Ruiz-Arias JA, Arbizu-Barrena C, Santos-Alamillos FJ, Tovar-Pescador J, Pozo-Vázquez D (2016) Assessing the surface solar radiation budget in the WRF model: A spatiotemporal analysis of the bias and its causes. Mon Weather Rev 144(2):703–711. https://doi.org/10.1175/MWR-D-15-0262.1

Ryu YH, Hodzic A, Descombes G, Hu M, Barré J (2019) Toward a better regional ozone forecast over CONUS using rapid data assimilation of clouds and meteorology in WRF-Chem. J Geophys Res 124(23):13576–13592. https://doi.org/10.1029/2019JD031232

Rzeszutek M, Kłosowska A, Oleniacz R (2023) Accuracy Assessment of WRF Model in the Context of Air Quality Modeling in Complex Terrain. Sustainability 15(16):12576. https://doi.org/10.3390/su151612576

Salva J, Poništ J, Rasulov O, Schwarz M, Vanek M, Sečkár M (2023) The impact of heating systems scenarios on air pollution at selected residential zone: a case study using AERMOD dispersion model. Environ Sci Eur 35(1):91. https://doi.org/10.1186/s12302-023-00798-1

Schorcht F, Kourti I, Scalet BM, Roudier S, Sancho LD (2013) Best available techniques (BAT) reference document for the production of cement, lime and magnesium oxide – Industrial Emissions Directive 2010/75/EU (integrated pollution prevention and control). Publications Office. https://doi.org/10.2788/12850

Schuhmacher M, Domingo JL, Garreta J (2004) Pollutants emitted by a cement plant: health risks for the population living in the neighborhood. Environ Res 95(2):198–206. https://doi.org/10.1016/j.envres.2003.08.011

Scire JS, Strimaitis DG, Yamartino RJ (2000) A user's guide for the CALPUFF dispersion model. Earth Tech, Inc 521:1–521

Shen W, Liu Y, Yan B, Wang J, He P, Zhou C, Huo X, Zhang W, Xu G, Ding Q (2017) Cement industry of China: Driving force, environment impact and sustainable development. Renew Sust Energ Rev 75:618–628. https://doi.org/10.1016/j.rser.2016.11.033

Shimada S, Ohsawa T, Kogaki T, Steinfeld G, Heinemann D (2015) Effects of sea surface temperature accuracy on offshore wind resource assessment using a mesoscale model. Wind Energy 18(10):1839–1854. https://doi.org/10.1002/we.1796

Sierra-Vargas MP, Teran LM (2012) Air pollution: Impact and prevention. Respirology 17(7):1031–1038. https://doi.org/10.1111/j.1440-1843.2012.02213.x

Skamarock WC, Klemp JB, Dudhia J, Gill DO, Liu Z, Berner J, Wang W, Powers JG, Duda MG, Barker DM, Huang X-Y (2019) A description of the advanced research WRF model version 4.1 (No. NCAR/TN-556+STR). https://doi.org/10.5065/1dfh-6p97

Song Q, Chelton DB, Esbensen SK, Thum N, O'Neill LW (2009) Coupling between sea surface temperature and low-level winds in mesoscale numerical models. J Clim 22(1):146–164. https://doi.org/10.1175/2008JCLI2488.1

Stanek LW, Sacks JD, Dutton SJ, Dubois J-JB (2011) Attributing health effects to apportioned components and sources of particulate matter: an evaluation of collective results. Atmos Environ 45(32):5655–5663. https://doi.org/10.1016/j.atmosenv.2011.07.023

Stein AF, Isakov V, Godowitch J, Draxler RR (2007) A hybrid modeling approach to resolve pollutant concentrations in an urban area. Atmos Environ 41(40):9410–9426. https://doi.org/10.1016/j.atmosenv.2007.09.004

Su L, Yuan Z, Fung JC, Lau AK (2015) A comparison of HYSPLIT backward trajectories generated from two GDAS datasets. Sci Total Environ 506:527–537. https://doi.org/10.1016/j.scitotenv.2014.11.072

Tartakovsky D, Broday DM, Stern E (2013) Evaluation of AERMOD and CALPUFF for predicting ambient concentrations of total suspended particulate matter (TSP) emissions from a quarry in complex terrain. Environ Pollut 179:138–145. https://doi.org/10.1016/j.envpol.2013.04.023

Tian J, Liu R, Ding L, Guo L, Liu Q (2021) Evaluation of the WRF physical parameterisations for Typhoon rainstorm simulation in southeast coast of China. Atmos Res 247:105130. https://doi.org/10.1016/j.atmosres.2020.105130

Trinh TT, Trinh TT, Le TT, Nguyen TDH, Tu BM (2019) Temperature inversion and air pollution relationship, and its effects on human health in Hanoi City, Vietnam. Environ Geochem Health 41:929–937. https://doi.org/10.1007/s10653-018-0190-0

TUIK (2023) The population of provinces by years 2022–2023. https://data.tuik.gov.tr/Bulten/Index?p=49685. Accessed 10 Oct 2023

Tuy S, Lee HS, Chreng K (2022) Integrated assessment of offshore wind power potential using Weather Research and Forecast (WRF) downscaling with Sentinel-1 satellite imagery, optimal sites, annual energy production and equivalent CO2 reduction. Renew Sust Energ Rev 163:112501. https://doi.org/10.1016/j.rser.2022.112501

Ünal Z, Dinç U, Özen C, Toros H (2019) Air Pollution Forecasting for Ankara with Machine Learning Method. J Res Atmos Sci 1(1):42–48

US EPA (2000) Requirements for preparation, adoption, and submittalof state implementation plans (Guideline on Air Quality Models); proposed rule. https://www.govinfo.gov/content/pkg/FR-2000-04-21/pdf/00-4235.pdf. Accessed 21 Mar 2024

US EPA (2009) Risk Assessment Guidance for Superfund Volume I: Human Health Evaluation Manual (Part F, Supplemental Guidance for Inhalation Risk Assessment). https://www.epa.gov/sites/default/files/2015-09/documents/partf_200901_final.pdf. Accessed 21 Mar 2024
US EPA (2019) AERMOD Implementation Guide. US Environmental Protection Agency. Ofce of Air Quality Planning and Standards. Emissions Monitoring and Analysis Division. Research Triangle Park https://nepis.epa.gov/Exe/ZyPURL.cgi?Dockey=P100XNK2.txt. Accessed 21 Mar 2024
USGS (2023) Mineral commodity summaries U.S. Geological survey https://pubs.usgs.gov/periodicals/mcs2023/mcs2023.pdf. Accessed 21 Mar 2024
Valappil VK, Kedia S, Dwivedi AK, Pokale SS, Islam S, Khare MK (2023) Assessing the performance of WRF ARW model in simulating heavy rainfall events over the Pune region: in support of operational applications. Meteorog Atmos Phys 135(2):16. https://doi.org/10.1007/s00703-023-00952-7
Verma SS, Desai B (2008) Effect of meteorological conditions on air pollution of Surat city. J Int Environ Appl Sci 3(5):358–367
Wang S, Chen B (2016) Accounting of SO2 emissions from combustion in industrial boilers. Energy Procedia 88:325–329. https://doi.org/10.1016/j.egypro.2016.06.141
Wang S, Xing J, Jang C, Zhu Y, Fu JS, Hao J (2011) Impact assessment of ammonia emissions on inorganic aerosols in East China using response surface modeling technique. Environ Sci Technol 45(21):9293–9300. https://doi.org/10.1021/es2022347
Weil J, Sykes R, Venkatram A (1992) Evaluating air-quality models: review and outlook. J Appl Meteorol Climatol 31(10):1121–1145. https://doi.org/10.1175/1520-0450(1992)031<1121:EAQMRA>2.0.CO;2
Wyszogrodzki AA, Liu Y, Jacobs N, Childs P, Zhang Y, Roux G, Warner TT (2013) Analysis of the surface temperature and wind forecast errors of the NCAR-AirDat operational CONUS 4-km WRF forecasting system. Meteorog Atmos Phys 122:125–143. https://doi.org/10.1007/s00703-013-0281-5
Zanobetti A, Schwartz J (2009) The effect of fine and coarse particulate air pollution on mortality: a national analysis. Environ Health Perspect 117(6):898–903. https://doi.org/10.1289/ehp.0800108
Zeydan Ö, Karademir A (2023) Comparison of two air quality models in complex terrain near seashore. Atmósfera 37:113–130. https://doi.org/10.20937/ATM.53118
Zhang K, Batterman S (2013) Air pollution and health risks due to vehicle traffic. Sci Total Environ 450-451:307–316. https://doi.org/10.1016/j.scitotenv.2013.01.074
Zhang Q, Wang Y, Ma Q, Yao Y, Xie Y, He K (2015) Regional differences in Chinese SO2 emission control efficiency and policy implications. Atmos Chem Phys 15(11):6521–6533. https://doi.org/10.5194/acp-15-6521-2015
Zhao B, Wang S, Liu H, Xu J, Fu K, Klimont Z, Hao J, He K, Cofala J, Amann M (2013) NOx emissions in China: historical trends and future perspectives. Atmos Chem Phys 13(19):9869–9897. https://doi.org/10.5194/acp-13-9869-2013
Zhao X, Zhou W, Han L (2019) Human activities and urban air pollution in Chinese mega city: An insight of ozone weekend effect in Beijing. Phys Chem Earth 110:109–116. https://doi.org/10.1016/j.pce.2018.11.005
Zhou Y, Levy JI, Hammitt JK, Evans JS (2003) Estimating population exposure to power plant emissions using CALPUFF: a case study in Beijing, China. Atmos Environ 37(6):815–826. https://doi.org/10.1016/S1352-2310(02)00937-8
Zou B, Zhan F, Zeng Y, Yorke C, Liu X (2011) Performance of kriging and EWPM for relative air pollution exposure risk assessment. Int J Environ Res 5(3):769–778. https://doi.org/10.22059/ijer.2011.383